AD-A035 698 JAYCOR DEL MAR CALIF F/G 12/1
A BALANCED EXPANSION TECHNIQUE FOR CONSTRUCTING ACCURATE FINITE--ETC(U)
FEB 77 R K CHAN N00014-76-C-0455
UNCLASSIFIED J77-75008-TR-1 NL

1 OF 1
AD A035698

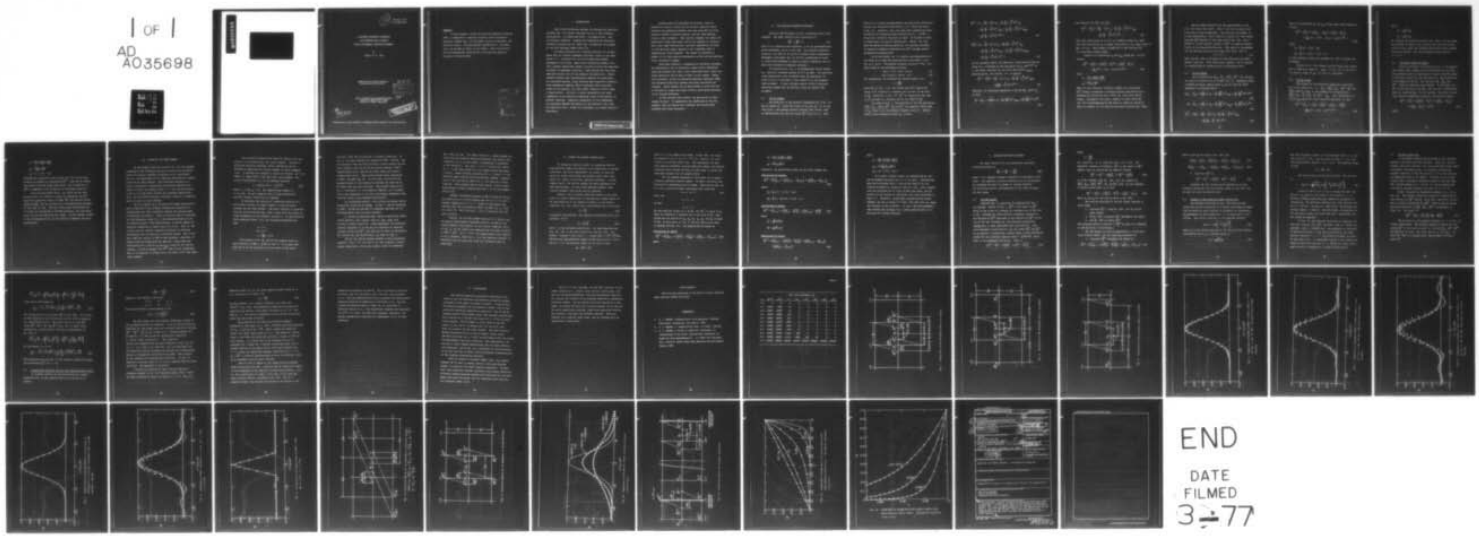

END
DATE FILMED
3-77

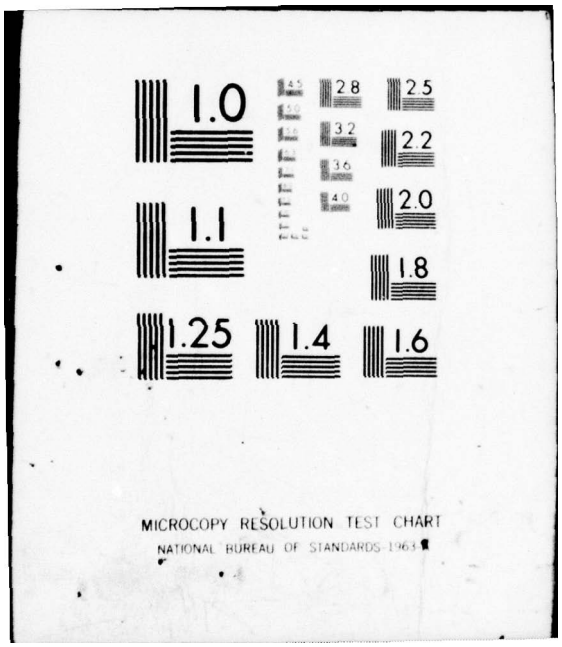
1.0
1.1
1.25
1.4
1.6
2.8
3.2
3.6
4.0
2.5
2.2
2.0
1.8
MICROCOPY RESOLUTION TEST CHART
NATIONAL BUREAU OF STANDARDS-1963

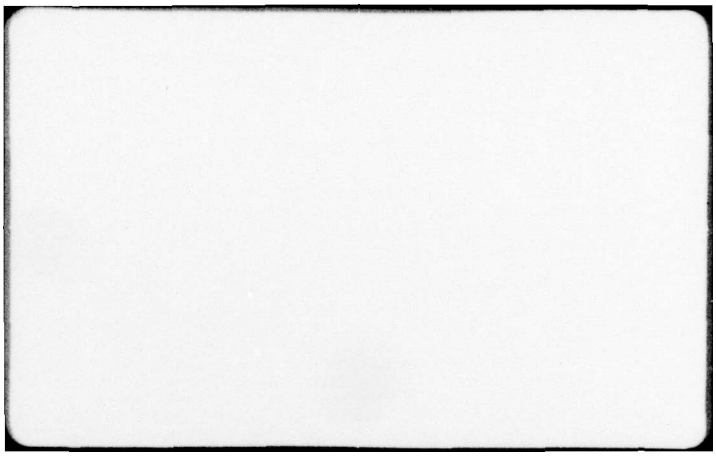

(12)

February 1977
J77-75008-TR-1

A BALANCED EXPANSION TECHNIQUE FOR CONSTRUCTING ACCURATE FINITE DIFFERENCE ADVECTION SCHEMES*

by

Robert K.-C. Chan

This research was sponsored under
Contract N00014-76-C-0455
Office of Naval Research

*Submitted to The Journal of Computational Physics for publication.

ABSTRACT

A new procedure, called the Balanced Expansion Technique (BET), is employed to construct accurate finite difference advection schemes that, for the model equation considered, are neutrally stable. By applying BET systematically, the phase error can be made as small as one wishes. Test calculations with one-dimensional problems have confirmed the expected accuracy of these methods.

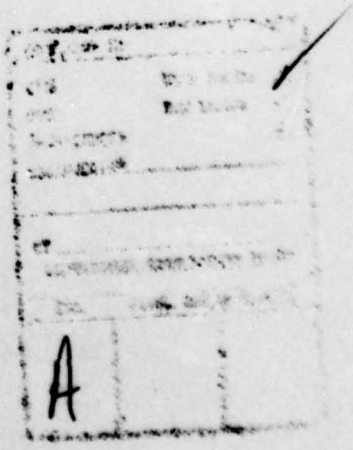

I. INTRODUCTION

Most finite difference methods for solving the advection equation (Eq. (1)) suffer from some or all of the following difficulties: (1) amplitude error, (2) phase error, and (3) Courant condition. Methods for simulating the advection-diffusion process (see Eq. (26)) may, in addition, be plagued by the cell Reynolds number limit {1}.

For pure convection at a constant velocity, it is well-known that all Fourier component solutions travel at the same speed (i.e., nondispersive) and their amplitudes remain unchanged at all times. Many finite difference schemes, however, produce significant amount of errors in both the amplitude and phase of component solutions. Some methods are free from amplitude errors, but do not preserve the phase well. While unstable schemes that systematically magnify the amplitudes are obviously useless, those deriving their numerical stability from nonphysical damping, which overwhelms other important terms in the equation, are also rather limited in their range of applications. Accuracy in phase preservation for those components in the physically important range of wavelengths is equally important. Numerical dispersion of such components can seriously degrade the quality of the solution, and, like the amplitude error, though less obviously, is a major source of inaccuracy.

Besides amplitude and phase distortions, explicit methods are usually limited by the Courant condition which restricts the maximum allowable time step such that no fluid particle travels a distance greater than one mesh spacing within a time increment. Some implicit schemes are stable for arbitrarily large time steps, but at the expense of accuracy. Thus, with these difficulties, accurate computation of flows at high Reynolds number appears to be a hopeless task in computational fluid dynamics. The reader is referred to Roache {1} for more detailed discussion on the various existing finite difference schemes.

This paper presents a fundamentally different procedure for developing a set of relatively simple finite difference advection schemes that lead to zero amplitude error, while the phase distortion can be made as small as one wishes. Using this procedure, called the Balanced Expansion Technique (BET), four different advection schemes have been constructed as examples. These schemes can be generalized to allow the use of arbitrarily large time steps, without sacrificing accuracy, and to include diffusion.

In the sections that follow, the derivation of each scheme is given. To demonstrate the usefulness of the new schemes, they are tested with transient and steady-state problems with known solutions.

II. THE BALANCED EXPANSION TECHNIQUE

The basic BET procedure is best illustrated with a few examples. The model equation that concerns us is

$$\frac{\partial \phi}{\partial t} + u \frac{\partial \phi}{\partial x} = 0 \qquad (1)$$

where ϕ is a passive scalar quantity, x is the one-dimensional space coordinate, and t is the time. The constant advection velocity u is taken to be positive without loss of generality. Throughout this paper, Eq. (1) will be interpreted in terms of fluid flows although it plays an equally important role in many other branches of physical sciences.

To discretize Eq. (1), a one-dimensional finite difference mesh with constant spacing δx will be used. The subscript j and superscript n are so defined that ϕ_j^n represents the value of ϕ at $x = j\delta x$ and $t = n\delta t$, where δt is the constant time increment. In what follows, several finite difference advection schemes will be derived, using the general BET procedure.

2.1 The A1 Scheme

The objective of any discrete representation of Eq. (1) may be stated as: Given the values of ϕ_j (for all j), at the time level n and perhaps several previous time levels, find an approximation for the new values ϕ_j^{n+1} (for all j). This

objective is usually accomplished by writing finite difference analogs for the partial derivatives, i.e., $\partial\phi/\partial t$ and $\partial\phi/\partial x$, in Eq. (1). Recently, some very high order schemes have been developed for evaluating these derivatives {1}. In BET, a drastically different approach is taken. No attempt is made to approximate the partial derivatives. Rather, one just uses the physical meaning behind Eq. (1) and then proceeds to obtain an algebraic expression for ϕ_j^{n+1} through careful mathematical manipulations.

As is well-known, Eq. (1) implies the preservation of the value of ϕ along the characteristic line $dx/dt = u$ in the (x,t) space. The general solution is $\phi(x,t) = F(x - ut)$, which leads to the following relations

$$\phi(x,t + \delta t) = \phi(x - u\delta t,t) \qquad (2)$$

$$\phi(x + u\delta t,t) = \phi(x,t - \delta t) \ . \qquad (3)$$

For convenience, we introduce the Courant number α as

$$\alpha \equiv \frac{u\delta t}{\delta x} \ . \qquad (4)$$

Referring to Fig. 1, Eq. (2) states that ϕ_j^{n+1} equals the value of ϕ^n located at a distance $u\delta t$ (or $\alpha\delta x$) to the left of ϕ_j^n. Similarly, by Eq. (3), ϕ_j^{n-1} is numerically the same as ϕ^n situated at a distance $\alpha\delta x$ to the right of ϕ_j^n.

As shown in Fig. 1, the positions of the six quantities ϕ_{j-1}^{n+1}, ϕ_{j-1}^{n}, ϕ_{j-1}^{n-1}, ϕ_j^{n+1}, ϕ_j^n, and ϕ_j^{n-1} are symmetric about that of ϕ_o, which is at the midpoint between j and j-1. Making Taylor series expansions about ϕ_o, we have

$$\phi_j^{n-1} = \phi_o + \left(\frac{1}{2} + \alpha\right)\delta x\ \phi_x + \frac{1}{2!}\left(\frac{1}{2} + \alpha\right)^2 \delta x^2\ \phi_{xx}$$

$$+ \frac{1}{3!}\left(\frac{1}{2} + \alpha\right)^3 \delta x^3\ \phi_{xxx} + \frac{1}{4!}\left(\frac{1}{2} + \alpha\right)^4 \delta x^4\ \phi_{xxxx}$$

$$+ \frac{1}{5!}\left(\frac{1}{2} + \alpha\right)^5 \delta x^5\ \phi^{(5)} + \ldots \qquad (5)$$

$$\phi_{j-1}^{n+1} = \phi_o - \left(\frac{1}{2} + \alpha\right)\delta x\ \phi_x + \frac{1}{2!}\left(\frac{1}{2} + \alpha\right)^2 \delta x^2\ \phi_{xx}$$

$$- \frac{1}{3!}\left(\frac{1}{2} + \alpha\right)^3 \delta x^3\ \phi_{xxx} + \frac{1}{4!}\left(\frac{1}{2} + \alpha\right)^4 \delta x^4\ \phi_{xxxx}$$

$$- \frac{1}{5!}\left(\frac{1}{2} + \alpha\right)^5 \delta x^5\ \phi^{(5)} + \ldots \qquad (6)$$

In the equations above, the subscript x means partial derivatives of ϕ, evaluated at the same point as ϕ_o, and $\phi^{(5)}$ is a shorthand notation for the fifth derivative ϕ_{xxxxx}. Subtracting Eq. (6) from Eq. (5), we obtain

$$\phi_j^{n-1} - \phi_{j-1}^{n+1} = 2\left(\frac{1}{2} + \alpha\right)\delta x\ \phi_x + \frac{2}{3!}\left(\frac{1}{2} + \alpha\right)^3 \delta x^3\ \phi_{xxx}$$

$$+ \frac{2}{5!}\left(\frac{1}{2} + \alpha\right)^5 \delta x^5\ \phi^{(5)} + \ldots \qquad (7)$$

Similarly, by combining expansions of ϕ_j^n and ϕ_{j-1}^n about ϕ_o, we have

$$\phi_j^n - \phi_{j-1}^n = 2\left(\frac{1}{2}\right)\delta x\ \phi_x + \frac{2}{3!}\left(\frac{1}{2}\right)^3 \delta x^3\ \phi_{xxx} + \frac{2}{5!}\left(\frac{1}{2}\right)^5 \delta x^5\ \phi^{(5)}$$

$$+ \ldots \qquad (8)$$

And likewise for ϕ_j^{n+1} and ϕ_{j-1}^{n-1},

$$\phi_j^{n+1} - \phi_{j-1}^{n-1} = 2\left(\frac{1}{2} - \alpha\right)\delta x\ \phi_x + \frac{2}{3!}\left(\frac{1}{2} - \alpha\right)^3 \delta x^3\ \phi_{xxx} + \frac{2}{5!}\left(\frac{1}{2} - \alpha\right)^5 \delta x^5\ \phi^{(5)} + \ldots \qquad (9)$$

Note that these pairs of ϕ's are all symmetric about ϕ_o, such that even derivatives of ϕ vanish identically on the right sides of Eqs. (7)-(9). This design is essential in the construction of a neutrally stable scheme.

Finally, by eliminating ϕ_x and ϕ_{xxx} among Eqs. (7)-(9), we have

$$\phi_j^{n+1} = \phi_{j-1}^{n-1} + a_1\left(\phi_{j-1}^{n+1} - \phi_j^{n-1}\right) + a_2\left(\phi_j^n - \phi_{j-1}^n\right) + \frac{1}{60}\alpha^2(1 - \alpha)(1 - 2\alpha)\ \delta x^5\ \phi^{(5)} + \ldots \qquad (10)$$

where

$$a_1 = \frac{(1 - \alpha)(1 - 2\alpha)}{(1 + \alpha)(1 + 2\alpha)}$$

$$a_2 = \frac{2(1 - 2\alpha)}{1 + \alpha}$$

Thus, we have obtained a discrete formula for calculating ϕ_j^{n+1} without attempting to evaluate partial derivatives of ϕ. Dropping the truncation error terms, Eq. (10) gives the A1 scheme. Throughout this paper, schemes for pure advection (Eq. (1)) are designated by the letter A, while we use AD to refer to schemes for the advection-diffusion process (Eq. (26)).

The A1 scheme involves only two space points (j and j-1), but three time levels. Thus it can not be used at the first step of time integration. The two-level A3 scheme, to be described shortly, may be used as a starter for this scheme. Although ϕ_{j-1}^{n+1} appears on the right side of Eq. (10), the A1 scheme is a fully explicit method if ϕ_j^{n+1} is computed sequentially in the downstream direction. The radius of convergence for the infinite series on the right side of Eq. (10) is

$$0 \le \alpha \le 1 \quad . \tag{11}$$

Thus, for Eq. (10) to be valid, we are limited by the usual Courant condition. This restriction, however, can be removed in a generalized A1 scheme as will be presented later.

2.2 The A2 Scheme

The six quantities ϕ_{j-2}^{n}, ϕ_{j-1}^{n}, ϕ_{j-1}^{n-1}, ϕ_{j}^{n+1}, ϕ_{j}^{n}, and ϕ_{j+1}^{n} are used to construct the A2 scheme (Fig. 2). Expanding these variables in Taylor series about ϕ_o we can form the three symmetric (or balanced) pairs

$$\phi_{j+1}^{n} - \phi_{j-2}^{n} = 2\left(\frac{3}{2}\right) \delta x\, \phi_x + \frac{2}{3!}\left(\frac{3}{2}\right)^3 \delta x^3\, \phi_{xxx} + \frac{2}{5!}\left(\frac{3}{2}\right)^5 \delta x^5\, \phi^{(5)} + \ldots \tag{12}$$

$$\phi_{j}^{n} - \phi_{j-1}^{n} = 2\left(\frac{1}{2}\right) \delta x\, \phi_x + \frac{2}{3!}\left(\frac{1}{2}\right)^3 \delta x^3\, \phi_{xxx} + \frac{2}{5!}\left(\frac{1}{2}\right)^5 \delta x^5\, \phi^{(5)} + \ldots \tag{13}$$

$$\phi_{j}^{n+1} - \phi_{j-1}^{n-1} = 2\left(\frac{1}{2} - \alpha\right) \delta x\, \phi_x + \frac{2}{3!}\left(\frac{1}{2} - \alpha\right)^3 \delta x^3\, \phi_{xxx} + \frac{2}{5!}\left(\frac{1}{2} - \alpha\right)^5 \delta x^5\, \phi^{(5)} + \ldots \tag{14}$$

Again, by eliminating ϕ_x and ϕ_{xxx} among these three equations, we have

$$\phi_j^{n+1} = \phi_{j-1}^{n-1} + b_1\left(\phi_{j-2}^{n} - \phi_{j+1}^{n}\right) + b_2\left(\phi_j^{n} - \phi_{j-1}^{n}\right) + \frac{1}{120}\,\alpha(1-\alpha^2)(1-2\alpha)(2-\alpha)\delta x^5\,\phi^{(5)} + \ldots \tag{15}$$

where

$$b_1 = \frac{1}{6}\,\alpha(1-\alpha)(1-2\alpha)$$

$$b_2 = \frac{1}{2}\,(1-2\alpha)(1+\alpha)(2-\alpha) \quad .$$

If the truncation errors are dropped, Eq. (15) is called the A2 scheme.

Similar to A1, this formula involves three time levels and is completely explicit. Again, for Eq. (15) to be valid, the Courant condition Eq. (11) must be satisfied.

2.3 The A3 Scheme

This scheme is constructed by expanding a different set of six quantities, i.e., ϕ_{j-2}^{n}, ϕ_{j-1}^{n+1}, ϕ_{j-1}^{n}, ϕ_j^{n+1}, ϕ_j^{n}, and ϕ_{j+1}^{n+1}, about ϕ_o (Fig. 3) and forming the balanced pairs $\phi_{j+1}^{n+1} - \phi_{j-2}^{n}$, $\phi_j^{n} - \phi_{j-1}^{n+1}$, and $\phi_j^{n+1} - \phi_{j-1}^{n}$. Upon elimination of ϕ_x and ϕ_{xxx} among the three resulting equations, we have

$$\phi_j^{n+1} = \phi_{j-1}^{n} + c_1\left(\phi_j^{n} - \phi_{j-1}^{n+1}\right) + c_2\left(\phi_{j-2}^{n} - \phi_{j+1}^{n+1}\right) + \frac{1}{120}\,\alpha(1-\alpha)(2-\alpha)\delta x^5\,\phi^{(5)} + \ldots \tag{16}$$

where

$$c_1 = \frac{2 - \alpha}{2(1 + \alpha)}$$

$$c_2 = \frac{\alpha}{2(3 - \alpha)} \quad .$$

By dropping the truncation errors, Eq. (16) is the A3 scheme. This method is implicit but involves only two time levels, which is very useful for starting other multi-level schemes such as A1 and A2. For the A3 scheme we also require $0 \leq \alpha \leq 1$.

2.4 The Higher Order A4 Scheme

From the principle illustrated so far, it is apparent that higher order schemes can be constructed by involving more balanced pairs of discretized ϕ values, with the center of each pair located at the same point ϕ_o. One possibility is to combine A1 and A2. The two pairs $\phi_j^n - \phi_{j-1}^n$ and $\phi_j^{n+1} - \phi_{j-1}^{n-1}$ are shared by both schemes. In fact Eqs. (8) and (9) are identical with Eqs. (13) and (14), respectively. Thus, by combining Eqs. (7)-(9) and Eqs. (12)-(14), we have four linearly independent equations from which we obtain

$$\phi_j^{n+1} = \phi_{j-1}^{n-1} + d_1\left(\phi_{j-1}^{n+1} - \phi_j^{n-1}\right) + d_2\left(\phi_{j+1}^{n} - \phi_{j-2}^{n}\right) + d_3\left(\phi_j^n - \phi_{j-1}^n\right) + O(\delta x^7) \qquad (17)$$

where

$$d_1 = \frac{(2 - \alpha)(1 - 2\alpha)}{(2 + \alpha)(1 + 2\alpha)}$$

$$d_2 = \frac{\alpha^2(1 - 2\alpha)}{3(2 + \alpha)}$$

$$d_3 = (2 - \alpha)(1 - 2\alpha)$$

Dropping the truncation errors terms, Eq. (17) is the very accurate A4 scheme for calculating ϕ_j^{n+1}. Like the A1 scheme, this method involves three time levels, but is explicit if ϕ_j^{n+1} is computed in the direction of increasing value of j.

From the development above, one could use one more balanced pair of ϕ values to obtain an expression for ϕ_j^{n+1} which has truncation errors of order δx^9, the new pair being ϕ_{j-2}^{n-1} and ϕ_{j+1}^{n+1}, and the process can be systematically extended to any order we wish. The more lower-order odd derivatives of ϕ that are eliminated in the BET procedure, the less phase error will be introduced by the scheme. As will become evident in the following section, the A4 scheme is adequate for most applications.

III. STABILITY AND PHASE ERRORS

By von Neumann stability analysis {1}, all the schemes presented in the preceding section are found to be neutrally stable for Fourier component solutions of all wavelengths. That is, the amplitudes of the component solutions are exactly preserved by these schemes. This desirable property is a direct consequence of employing the balanced expansion procedure in which the damping terms (i.e., all the even derivatives of ϕ in the Taylor series) are cancelled identically. Thus, the so-called artificial viscosity, explicit or implicit, does not exist in these schemes.

We are slightly less fortunate with phase preservation. Exact solutions of the original differential equation (1) should advect all wave components through the discrete mesh at precisely the speed u. Since we were not able to eliminate all the dispersion terms (i.e., the odd derivatives of ϕ in the Taylor series) in the BET procedure, a certain amount of numerical dispersion or phase error will occur. That is, for a given size δx, Fourier component solutions of different wavelengths will be advected at different speeds. One of the most important aspects of BET is the systematic reduction of phase errors by eliminating the dominant, lower-order odd derivatives of ϕ, such as ϕ_x and ϕ_{xxx} in the A1, A2, and A3 schemes. In the A4 scheme, the $\phi^{(5)}$ term is also eliminated. Thus it is expected to produce even less phase error than these other schemes.

The analysis of phase error based on Fourier wave components is straightforward, but rather lengthy. Instead of giving the detailed analyses, useful information can be obtained by employing the various schemes in actual computations. A standard test problem is chosen as follows: At t = 0 (NCYC = 0, where NCYC is the time level cycle number), the initial distribution of ϕ is the Gaussian function

$$\phi = \exp\{(\ln 2)(x - x_o)^2/r^2\} \qquad (18)$$

where r = 5 and x_o = 30. The computational domain is $0 \leq x \leq 60$. To save computer time in long calculations, periodic boundary conditions are imposed.

To determine the quality of a numerical solution at a given point in time, we simply compare it with the exact solution for the same instant. The exact solution is identical with the initial profile (Eq. (18)), except with the center x_o being transported at the constant velocity u. In the series of tests conducted (Figs. 4-7), the following parameters are used

$$u = 1.0$$

$$\delta x = 1.0$$

$$\alpha = \frac{u\delta t}{\delta x} = 0.75 \quad .$$

The results of A1, A2, and A3 are compared with the exact solution at NCYC = 10,000 in Fig. 4. It is seen that both the A1 and A2 solutions are very close to the exact

solution, while the A3 solution is slightly distorted. In Fig. 5, the three schemes are compared at NCYC = 20,000. Now the deviation from the exact solution is more visible for all three schemes, with the A1 and A2 results showing a small lagging phase error, and the A3 result definitely shows a leading phase error. These errors become quite pronounced at NCYC = 50,000 (Fig. 6). At this time, notice that the maximum heights of the numerical solutions are about 4% to 6% lower than the exact solution. This height reduction is not a consequence of any numerical damping, but is rather due to the dispersion of the short wavelength components away from the center of the Gaussian distribution.

As anticipated earlier, very accurate solutions can be obtained by using the A4 scheme. In Fig. 7, the A4 solutions at NCYC = 50,000 and 100,000 are compared, and they are indistinguishable from the exact solution.

It should be mentioned that, while A1 and A4 are effectively explicit, they become implicit when used with periodic boundary conditions. From experience, an economical solution procedure is to use A2 as a predictor to find provisional values for ϕ_j^{n+1}, and then use A4 twice as correctors. The results are very satisfactory, as shown in Fig. 7.

The A1, A2, and A4 schemes possess a very interesting property: For $\alpha = 0$, 1/2, and 1, all the truncation errors vanich identically, as one can readily verify by examining

Eqs. (10) and (15). For those values of α, these schemes are exact and they preserve absolutely whatever the initial distribution of ϕ is in the domain, transporting it precisely at the velocity u. The case $\alpha = 0$ is a trivial one, while for $\alpha = 1$ the mesh values of ϕ are simply passed from point to point. These limiting properties for $\alpha = 0$ and $\alpha = 1$ are shared by many existing finite difference schemes. However, that A1, A2, and A4 are exact for $\alpha = 1/2$ came as a little surprise. This property may be quite useful, since in most applications δt may be chosen such that α is in the neighborhood of 1/2.

Another interesting finding is that in both A1 and A2, the phase error is of the leading type for $0 \leq \alpha \leq \frac{1}{2}$, and it becomes lagging for $\frac{1}{2} \leq \alpha \leq 1$. Figure 8 illustrates this behavior with the A2 results at NCYC = 50,000, for $\alpha = 0.25$, 0.5, and 0.75. The curve for $\alpha = 0.5$ is identical with the exact solution.

Finally, the various schemes were put to a severe test by using a sharp-peaked triangular profile, instead of the smooth Gaussian distribution, as the initial condition for ϕ. In Fig. 9, the A2 results are compared with the exact solution at NCYC = 1400. For $\alpha = 0.75$, the lagging phase error typical of A2 is apparent, while for $\alpha = 0.5$ the numerical solution is identical with the exact one (even the triangular peak is preserved).

IV. BEYOND THE COURANT NUMBER LIMIT

To design an accurate scheme for computing flows at high Reynolds number (see Section V for extensions to include diffusion), the first requirement, of course, is that the advection scheme itself does not produce errors that overwhelm the effect of the real, physical diffusion. In this regard, the A1, A2, and A3 schemes are good candidates for such applications. At very large Reynolds numbers, more accurate schemes, such as A4, may be required.

However, even a perfect advection scheme is not sufficient for actual computation of high Reynolds number flows, if the applicability of the scheme is subject to the Courant condition, Eq. (11), which limits the maximum size of δt to be

$$\delta t \leq \frac{\delta x}{u} \quad . \tag{19}$$

In explicit calculations, the stability restriction on δt for diffusion {1} is

$$\delta t \leq \frac{1}{2} \frac{\delta x^2}{\nu} \tag{20}$$

where ν is the diffusion coefficient. At large Reynolds numbers, Eq. (19) is far more restrictive than Eq. (20). For example, consider a flow with $u = 1$ ft/sec and $\nu = 10^{-5}$ ft^2/sec. Assuming the characteristic length of the flow to be $D = 10$ ft, and $\delta x = 1$ ft, the Reynolds number of the flow is then

$$Re = \frac{uD}{\nu} = 10^6$$

which is a very common flow regime. By Eq. (20), one would be allowed to use δt up to 5×10^4 sec; however, Eq. (19) limits δt to be less than 1 sec. The consequence is that, even using an extremely accurate advection scheme, the Courant condition would require millions of time steps to obtain any meaningful results for the example above.

All the schemes presented in this paper can be generalized to arbitrary Courant number. We shall illustrate the principle by considering the A1 scheme. Referring to Fig. 10, let s be a positive integer (including zero) such that

$$s \leq \alpha < s + 1 \quad . \tag{21}$$

Also, let

$$\alpha' \equiv \alpha - s$$

so that

$$0 \leq \alpha' < 1$$

For any positive values of α, by Eq. (2) ϕ_j^{n+1} is equal to ϕ_D which is located at a distance $\alpha\delta x$ to the left of ϕ_j^n. Comparing the six quantities ϕ_A, ϕ_B, ϕ_C, ϕ_D, ϕ_E, and ϕ_F as shown in Fig. 10 with those in Fig. 1, one can easily write down, in analogy with Eq. (10), the generalized A1 scheme as

<u>Generalized A1 Scheme</u>

$$\phi_j^{n+1} = \phi_{j-2s-1}^{n-1} + a_1'\left(\phi_{j-1}^{n+1} - \phi_{j-2s}^{n-1}\right) + a_2'\left(\phi_{j-s}^{n} - \phi_{j-s-1}^{n}\right) \tag{22}$$

where

$$a_1' = \frac{(1 - \alpha')(1 - 2\alpha')}{(1 + \alpha')(1 + 2\alpha')}$$

$$a_2' = \frac{2(1 - 2\alpha')}{1 + \alpha'}$$

Similarly, the generalized forms for the other schemes are

Generalized A2 Schemes

$$\phi_j^{n+1} = \phi_{j-2s-1}^{n-1} + b_1'\left(\phi_{j-s-2}^{n} - \phi_{j-s+1}^{n}\right) + b_2'\left(\phi_{j-s}^{n} - \phi_{j-s-1}^{n}\right) \tag{23}$$

where

$$b_1' = \frac{1}{6}\,\alpha'(1 - \alpha')(1 - 2\alpha')$$

$$b_2' = \frac{1}{2}\,(1 - 2\alpha')(1 + \alpha')(2 - \alpha')$$

Generalized A3 Scheme

$$\phi_j^{n+1} = \phi_{j-s-1}^{n} + c_1'\left(\phi_{j-s}^{n} - \phi_{j-1}^{n+1}\right) + c_2'\left(\phi_{j-s-2}^{n} - \phi_{j+1}^{n+1}\right) \tag{24}$$

where

$$c_1' = \frac{2 - \alpha'}{2(1 + \alpha')}$$

$$c_2' = \frac{\alpha'}{2(3 - \alpha')}$$

Generalized A4 Scheme

$$\phi_j^{n+1} = \phi_{j-2s-1}^{n-1} + d_1'\left(\phi_{j-1}^{n+1} - \phi_{j-2s}^{n-1}\right) + d_2'\left(\phi_{j-s+1}^{n} - \phi_{j-s-2}^{n}\right) + d_3'\left(\phi_{j-s}^{n} - \phi_{j-s-1}^{n}\right) \tag{25}$$

where

$$d_1' = \frac{(2 - \alpha')(1 - 2\alpha')}{(2 + \alpha')(1 + 2\alpha')}$$

$$d_2' = \frac{(\alpha')^2 (1 - 2\alpha')}{3(2 + \alpha')}$$

$$d_3' = (2 - \alpha')(1 - 2\alpha')$$

As in their original forms, the generalized A1, A2, and A4 schemes are exact for $\alpha' = 0$, $\frac{1}{2}$, and 1. Calculations have been performed with $\alpha = 100.75$ and 1000.75 for the problem discussed in connection with Eq. (18). Each computation was continued for at least 10,000 time steps, and the quality of the results is consistent with those mentioned in Figs. 4-7. Therefore, unlike many unconditionally stable schemes, the use of large δt in Eqs. (22)-(25) does not impair the accuracy of the solutions. In fact, the only parameter that affects the accuracy (i.e., phase preservation) is α', the size of α being irrelevant.

V. ADVECTION-DIFFUSION SCHEMES

The model equation for one-dimensional advection-diffusion process is

$$\frac{\partial \phi}{\partial t} + u \frac{\partial \phi}{\partial x} = \nu \frac{\partial^2 \phi}{\partial x^2} \tag{26}$$

where ν is a constant kinematic viscosity or diffusion coefficient. The numerical solution procedure will be illustrated by extending the basic A1 scheme to include diffusion. The resulting discrete representation of Eq. (26) is called the AD1 scheme.

5.1 The AD1 Scheme

Consider Fig. 11, which may be compared with Fig. 1 for analogy. Unlike in Fig. 1, ϕ_j^{n+1} is not equal to $\tilde{\phi}_j^{n+1}$ which is the value of ϕ located at a distance $\alpha\delta x$ to the left of ϕ_j^n. Although the fluid particle originally situated at the location of $\tilde{\phi}_j^{n+1}$ does move to the position of ϕ_j^{n+1} at the end of the time increment δt, the diffusion process has changed the ϕ value associated with this particle. From this Lagrangian interpretation, one can relate $\tilde{\phi}_j^{n+1}$ and ϕ_j^{n+1} by an explicit, forward-time, central-space, finite difference scheme for the diffusion equation $D\phi/Dt = \nu(\partial^2\phi/\partial x^2)$, where D/Dt is the Lagrangian derivative. That is,

$$\phi_j^{n+1} = \tilde{\phi}_j^{n+1} + \beta\left(\tilde{\phi}_{j+1}^{n+1} - 2\,\tilde{\phi}_j^{n+1} + \tilde{\phi}_{j-1}^{n+1}\right) \tag{27}$$

where

$$\beta \equiv \frac{\nu \delta t}{\delta x^2} \quad .$$

For stability, it is required that $0 \leq \beta \leq 1/2$ {1}. Similarly, because of diffusion, ϕ_j^{n-1} is not equal to $\tilde{\phi}_j^{n-1}$. Rather, they are related by the explicit formula

$$\tilde{\phi}_j^{n-1} = \phi_j^{n-1} + \beta\left(\phi_{j+1}^{n-1} - 2\,\phi_j^{n-1} + \phi_{j-1}^{n-1}\right) \tag{28}$$

In close analogy with Eq. (10), the six quantities $\tilde{\phi}_{j-1}^{n+1}$, ϕ_{j-1}^{n}, $\tilde{\phi}_{j-1}^{n-1}$, $\tilde{\phi}_j^{n+1}$, ϕ_j^n, and $\tilde{\phi}_j^{n-1}$ (Fig. 11) are expanded in Taylor series about ϕ_o to give

$$\tilde{\phi}_j^{n+1} = \tilde{\phi}_{j-1}^{n-1} + a_1\left(\tilde{\phi}_{j-1}^{n+1} - \tilde{\phi}_j^{n-1}\right) + a_2\left(\phi_j^n - \phi_{j-1}^n\right) \tag{29}$$

where a_1 and a_2 are the same as given in Eq. (10).

The solution procedure in the AD1 scheme consists of three steps:

1. Calculate $\tilde{\phi}_j^{n-1}$, using Eq. (28), for the entire space domain.
2. By Eq. (29), calculate $\tilde{\phi}_j^{n+1}$ throughout the domain.
3. Use Eq. (27) to obtain ϕ_j^{n+1}.

The procedure above is explicit if $\tilde{\phi}_j^{n+1}$ in Step 2 is computed in the direction of increasing j.

The AD1 scheme can also be generalized to allow arbitrary Courant number, and the resulting procedure is

1. Calculate $\tilde{\phi}_j^{n+1}$ throughout the domain by

$$\tilde{\phi}_j^{n+1} = \tilde{\phi}_{j-2s-1}^{n-1} + a_1'\left(\tilde{\phi}_{j-1}^{n+1} - \tilde{\phi}_{j-2s}^{n-1}\right) + a_2'\left(\phi_{j-s}^n - \phi_{j-s-1}^n\right) \tag{30}$$

where a_1' and a_2' are given in Eq. (22), and

$$\tilde{\phi}^{n-1}_{j-2s} = \phi^{n-1}_{j-2s} + \beta\left(\phi^{n-1}_{j-2s+1} - 2\phi^{n-1}_{j-2s} + \phi^{n-1}_{j-2s-1}\right) \tag{31}$$

$$\tilde{\phi}^{n-1}_{j-2s-1} = \phi^{n-1}_{j-2s-1} + \beta\left(\phi^{n-1}_{j-2s} - 2\phi^{n-1}_{j-2s-1} + \phi^{n-1}_{j-2s-2}\right) . \tag{32}$$

2. Calculate ϕ^{n+1}_j by

$$\phi^{n+1}_j = \tilde{\phi}^{n+1}_j + \beta\left(\tilde{\phi}^{n+1}_{j+1} - 2\tilde{\phi}^{n+1}_j + \tilde{\phi}^{n+1}_{j-1}\right) . \tag{33}$$

Likewise, A2, A3, and A4 can be extended to include diffusion and allow arbitrary Courant number at the same time. We shall not give the details here.

5.2 Example of High Reynolds Number Calculation

The procedure described by Eqs. (30)-(33) has been tested with actual computation of a simple high Reynolds number flow for which an exact solution is available for comparison. The parameters of the problem are: $u = 1$ ft/sec and $\nu = 10^{-4}$ ft^2/sec. The initial condition is the Gaussian function

$$\phi(x,0) = \exp\left[-\frac{(x - x_o)^2}{4\nu t_o}\right] \tag{34}$$

where x_o is the initial position of the center of the Gaussian distribution and t_o is a constant given by

$$t_o = \frac{r^2}{4\nu(\ln 2)} . \tag{35}$$

The "half-strength" radius r is the distance from $x = x_o$ such that $\phi(x_o \pm r, 0) = 1/2$. For this test we used r = 5 ft, thus the characteristic length D = 2r = 10 ft. The Reynolds number is then

$$Re = \frac{uD}{\nu} = 10^5 \quad .$$

The exact solution which satisfies Eqs. (26) and (34) is

$$\phi(x,t) = \sqrt{\frac{t_o}{t + t_o}} \exp\left[- \frac{(x - x_o - ut)^2}{4\nu(t + t_o)} \right] \quad . \qquad (36)$$

A mesh of 100 δx (δx = 1 ft) in length was used, the point $x = x_o$ being at the center of this domain at t = 0. Periodic boundary conditions were imposed to economize the computation. For diffusion stability, Eq. (20) requires that $\delta t \leq 5 \times 10^3$ sec. We used δt = 1000.75 sec, which makes the Courant number α = 1000.75. The AD3 scheme, an extension of A3, was used to start the first time step. Afterwards, the AD1 scheme was employed.

In Fig. 12, the numerical solutions are compared with the exact solution, Eq. (36), for NCYC = 100 (t = 100075 sec) and NCYC = 360 (t = 360270 sec). The agreement is excellent. As mentioned earlier, if one were restricted by the usual Courant condition $0 \leq \alpha \leq 1$, the maximum allowable δt would be less than 1 sec. It would then take more than 100075 time steps to obtain the solution at t = 100075 sec, which would make the cost of computation a rather serious matter.

5.3 Boundary Conditions

In the sample calculations mentioned so far, periodic boundary conditions have been employed. There are, however, numerous advection-diffusion flow situations where other types of boundary conditions arise. A frequently encountered boundary condition is the specification of ϕ at the upstream and downstream ends of the domain. We shall limit our discussion here to boundary conditions needed in the basic AD1, AD2, and AD3 schemes (i.e., the A1, A2, and A3 schemes generalized to include diffusion, but only for $0 \leq \alpha \leq 1$).

First, consider the downstream boundary (at $j = R$ in Fig. 13). The boundary quantities needed for computation in the interior are $\tilde{\phi}_R^{n+1}$ and ϕ_R^n. Since ϕ_R^n is specified, we only have to find an expression for $\tilde{\phi}_R^{n+1}$. This is done by making balanced expansions of $\tilde{\phi}_{R-1}^{n+1}$, ϕ_{R-1}^n, $\tilde{\phi}_R^{n+1}$, and ϕ_R^n about ϕ_o (Fig. 13). The result is

$$\tilde{\phi}_R^{n+1} = \phi_{R-1}^n + \left(\frac{1 - \alpha}{1 + \alpha}\right)\left(\phi_R^n - \tilde{\phi}_{R-1}^{n+1}\right) \qquad (37)$$

The situation at the upstream boundary ($j = L$ in Fig. 13) is more complicated. The boundary quantities needed for computing ϕ_j^{n+1} at the interior point $j = L+1$ are ϕ_{L-1}^n, $\tilde{\phi}_L^{n-1}$, $\tilde{\phi}_L^{n+1}$, and ϕ_L^n which is known. The first step is to find ϕ_{L-1}^n. We write Eq. (26) in a forward-time, central-space difference about ϕ_L^n:

$$\frac{\phi_L^{n+1} - \phi_L^n}{\delta t} + u\left(\frac{\phi_{L+1}^n - \phi_{L-1}^n}{2\delta x}\right) = \nu\left(\frac{\phi_{L+1}^n - 2\phi_L^n + \phi_{L-1}^n}{\delta x^2}\right)$$

which can be rearranged as

$$\phi_{L-1}^n = \frac{(\alpha - 2\beta)\ \phi_{L+1}^n + 4\beta\ \phi_L^n + 2\left(\phi_L^{n+1} - \phi_L^n\right)}{\alpha + 2\beta} \quad . \qquad (38)$$

The second step is to calculate $\tilde{\phi}_L^{n-1}$ by Eq. (28). To do this, we need ϕ_{L-1}^{n-1} which can be obtained from Eq. (38) by reducing all superscripts by one. The third step is to find $\tilde{\phi}_L^{n+1}$. Using ϕ_L^{n+1}, $\tilde{\phi}_L^{n+1}$, ϕ_L^n, and $\tilde{\phi}_L^{n-1}$ (Fig. 13), we again form a forward-time, central-space, difference approximation to Eq. (26) as

$$\frac{\phi_L^{n+1} - \phi_L^n}{\delta t} + u\left(\frac{\tilde{\phi}_L^{n-1} - \tilde{\phi}_L^{n+1}}{2\alpha\ \delta x}\right) = \nu\left(\frac{\tilde{\phi}_L^{n-1} - 2\phi_L^n + \tilde{\phi}_L^{n+1}}{\alpha^2\ \delta x^2}\right)$$

By rearranging, we obtain

$$\tilde{\phi}_L^{n+1} = \frac{(\alpha^2 - 2\beta)\ \tilde{\phi}_L^{n-1} + 4\beta\ \phi_L^n + 2\alpha^2\left(\phi_L^{n+1} - \phi_L^n\right)}{\alpha^2 + 2\beta} \quad . \qquad (39)$$

The preceding steps provide all the boundary conditions needed for calculating ϕ_j^{n+1} at $j = L+1$.

5.4 Steady-State Solution and the Cell Reynolds Number Limit

To validate further the advection-diffusion schemes presented here, we have applied them to the steady-state problem

$$u \frac{\partial \phi}{\partial x} = \nu \frac{\partial^2 \phi}{\partial x^2} \qquad (40)$$

subject to the boundary conditions

$$\phi = 0 \qquad \text{at} \qquad x = 0$$

$$\phi = 1 \qquad \text{at} \qquad x = 1 \quad .$$

The exact solution to this problem is {2}

$$\phi(x) = \frac{1 - e^{(ux)/\nu}}{1 - e^{u/\nu}} \quad . \qquad (41)$$

The AD1 scheme with the boundary conditions treated in the preceding section was employed. A set of finite difference equations for the steady state was obtained from AD1 by setting $\phi_j^{n+1} = \phi_j^{n-1} = \phi_j^n$ for all values of j. Following Roache {2}, we used $\delta x = 0.1$ and solved the steady-state equations by direct Gauss elimination. The numerical results are compared with the exact solution in Fig. 14, for $\nu/u = \infty$, 1.0, 0.25, 0.10, and 0.05. For ν/u less than 0.10, the numerical solution becomes less accurate as ν/u decreases, because of inadequate resolution by the mesh. The accuracy can be improved by increasing the resolution. In Fig. 15, numerical solutions using $\delta x = 0.01$ are compared with the exact solutions. The agreement is excellent.

A difficulty suffered by many existing advection-diffusion schemes is the "cell Reynolds number limit," which has been described in detail by Roache {1, 2, 3}. The cell

Reynolds number (R_c) is the local Reynolds number based on δx as a characteristic length, viz.

$$R_c = \frac{u\delta x}{\nu} \quad . \tag{42}$$

In many schemes, e.g., central difference for $\partial\phi/\partial x$ and $\partial^2\phi/\partial x^2$ in Eq. (40), the steady-state numerical solutions are qualitatively similar to the exact solutions for $R_c \leq 2$. But when $R_c > 2$, the discrete solutions are oscillatory and diverge badly from the exact solutions.

Using any one of the advection-diffusion schemes presented in this paper (e.g., AD1), solutions have been obtained for $R_c > 2$ and up to $R_c = 10^8$. Table I shows the numerical results for those cases using $\delta x = 0.1$. The discrete ϕ values shown in the table have been multiplied by a factor of 10^5 for easy reading. It is seen that as R_c increases (or as ν/u decreases for a fixed δx), ϕ becomes vanishingly small over a greater portion of the domain and it rises more sharply near $x = 1$ to meet the downstream boundary condition $\phi(1) = 1$. At $R_c = 10^8$, a literally discontinuous solution is obtained, which is in agreement with the exact solution.

Since δx and δt appear in the steady-state difference equations derived from AD1, a question may be raised with regard to the uniqueness of the numerical steady-state solution. That is, for a given pair of u and ν ($u \neq 0$ and $\nu \neq 0$), only one exact solution exists, according to Eq. (41). But in a numerical model, the solution may depend on the choice of the

nonphysical parameters δx and δt. Once a suitable δx has been selected, then for the given u and ν the only free parameter is δt. Thus the question boils down to whether the steady-state numerical solution is sensitive to variation in δt. For the various calculations shown in Figs. 14, 15, and Table I, identical results (i.e., four significant figures) were obtained for $10^{-5} \leq \alpha \leq 0.99$. For practical purposes, therefore, the present steady-state solutions are independent of δt, as they should be.

VI. CONCLUSIONS

The various numerical experiments conducted so far indicate that the advection and advection-diffusion schemes presented in this paper are highly accurate. In particular, the advection schemes are all neutrally stable, free of any artificial viscosity (positive or negative). The A1 and A2 schemes produce little phase errors, and accurate results have been obtained up to 20,000 time steps (at $\alpha = 0.75$) by using either method. The A3 scheme is fully implicit and more costly to use, but it is needed only for the first time step as a starter for the other schemes. The most accurate method considered so far is the A4 scheme, which, after 100,000 time steps (at $\alpha = 0.75$), yields results that are hardly distinguishable from exact solutions. More importantly, the success of these schemes demonstrates that for some differential equations, such as Eq. (1), evaluation of the derivatives is not the only way to obtain finite difference representations of the original differential equation.

With the removal of Courant number limit, the present schemes can be used to compute flows at very high Reynolds number, at least for the model equation considered. Furthermore, with sufficient spatial resolution the present advection-diffusion schemes produced steady-state solutions that not only agree with exact solutions, but are completely free from the cell Reynolds number limit.

While it is true that Eqs. (1) and (26) represent fairly simple systems (i.e., linear, with constant coefficients, and only for one space dimension), they are nevertheless important for testing the validity of any proposed advection or advection-diffusion schemes. By the general principle described in this paper, the author believes that accurate schemes can be derived for multi-dimensional problems, flows with nonuniform velocity and viscosity, and mesh with variable spacings. These extensions are currently under study, and the findings will be reported at a future date.

Acknowledgment

This work was sponsored by the Office of Naval Research under Contract N00014-76-C-0455.

REFERENCES

1. P. J. ROACHE, "Computational Fluid Dynamics," Hermosa Publishers, Albuquerque, New Mexico, 1976.
2. P. J. ROACHE, J. Computational Phys. 10 (1972), 169-184.
3. P. J. ROACHE, A review of numerical techniques, in "Proceedings of the First International Conference on Numerical Ship Hydrodynamics." (J. Schot & N. Salvesen, Ed.), David W. Taylor Naval Ship Research and Development Center, 1975.

Table I

	Cell Reynolds Number R_c							
x	10^{-11}	10^{-1}	1	10	10^2	10^3	10^5	10^8
0.0	0	0	0	0	0	0	0	0
0.1	10000	6126	22	0	0	0	0	0
0.2	20000	12900	72	0	0	0	0	0
0.3	30000	20380	195	0	0	0	0	0
0.4	40000	28640	491	0	0	0	0	0
0.5	50000	37770	1205	0	0	0	0	0
0.6	60000	47870	2930	1	0	0	0	0
0.7	70000	59020	7093	12	0	0	0	0
0.8	80000	71340	17150	249	3	0	0	0
0.9	90000	84950	41410	4988	500	50	1	0
1.0	100000	100000	100000	100000	100000	100000	100000	100000

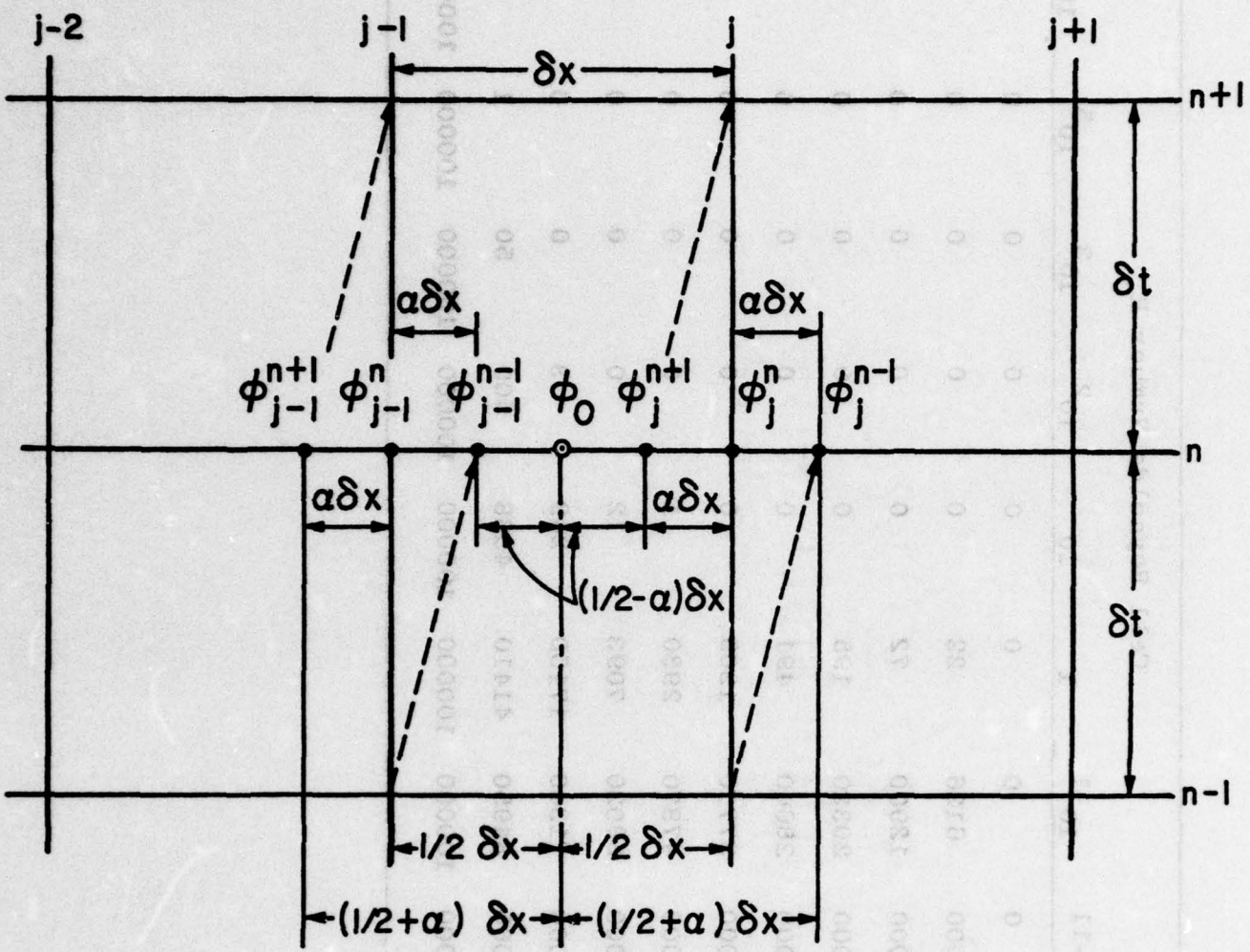

Fig. 1. Definition of the Variables Used in A1 Scheme.

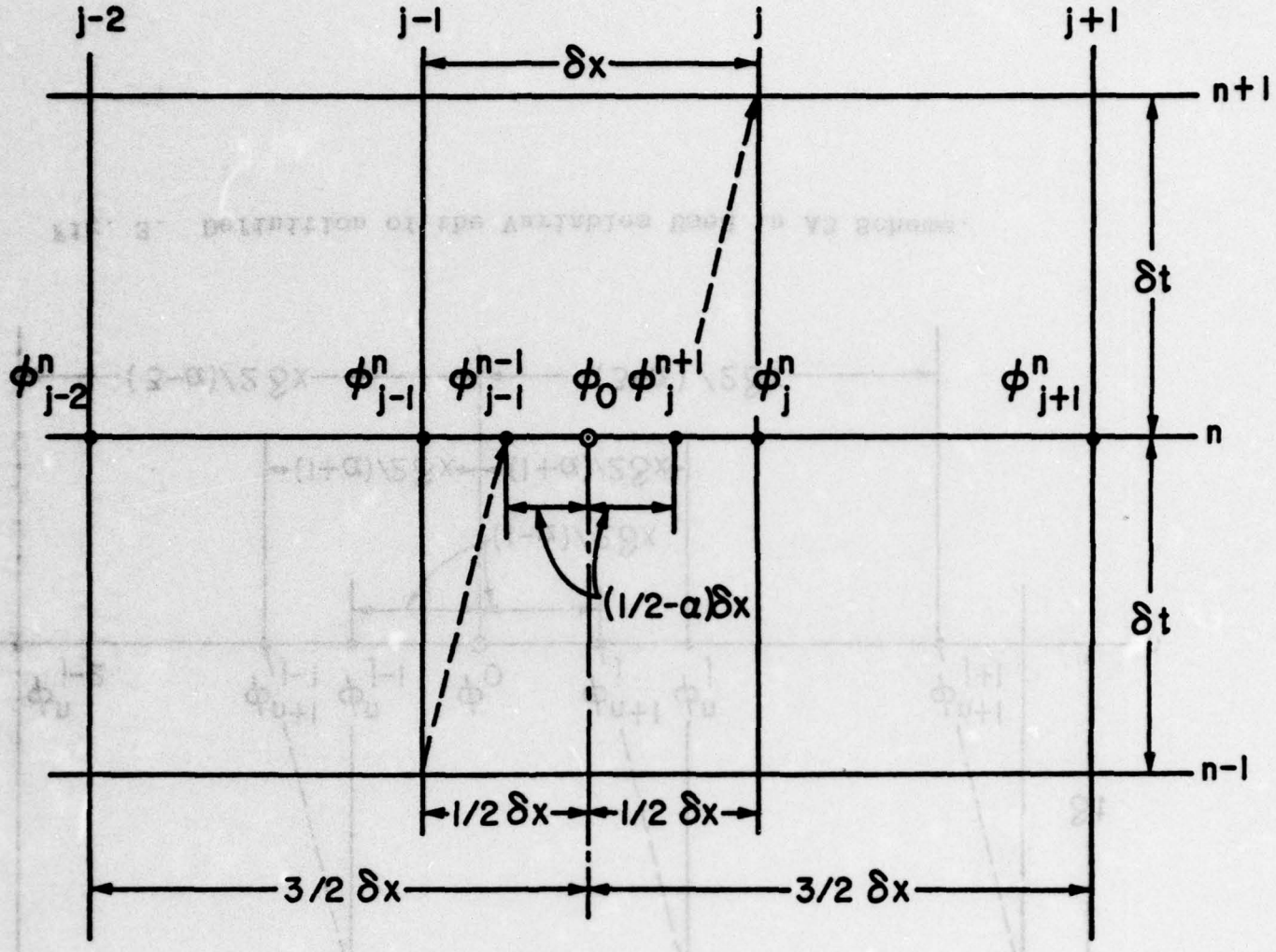

Fig. 2. Definition of the Variables Used in A2 Scheme.

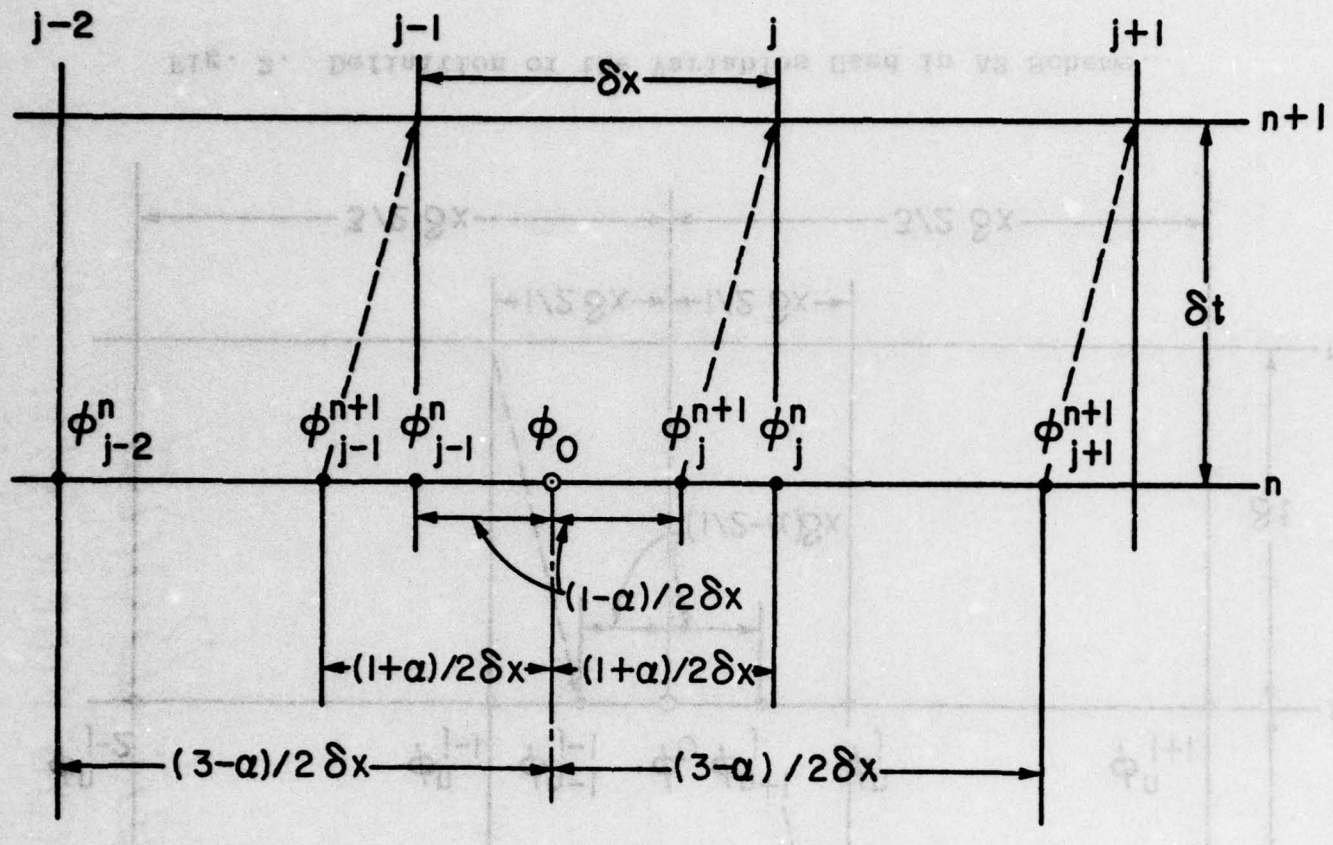

Fig. 3. Definition of the Variables Used in A3 Scheme.

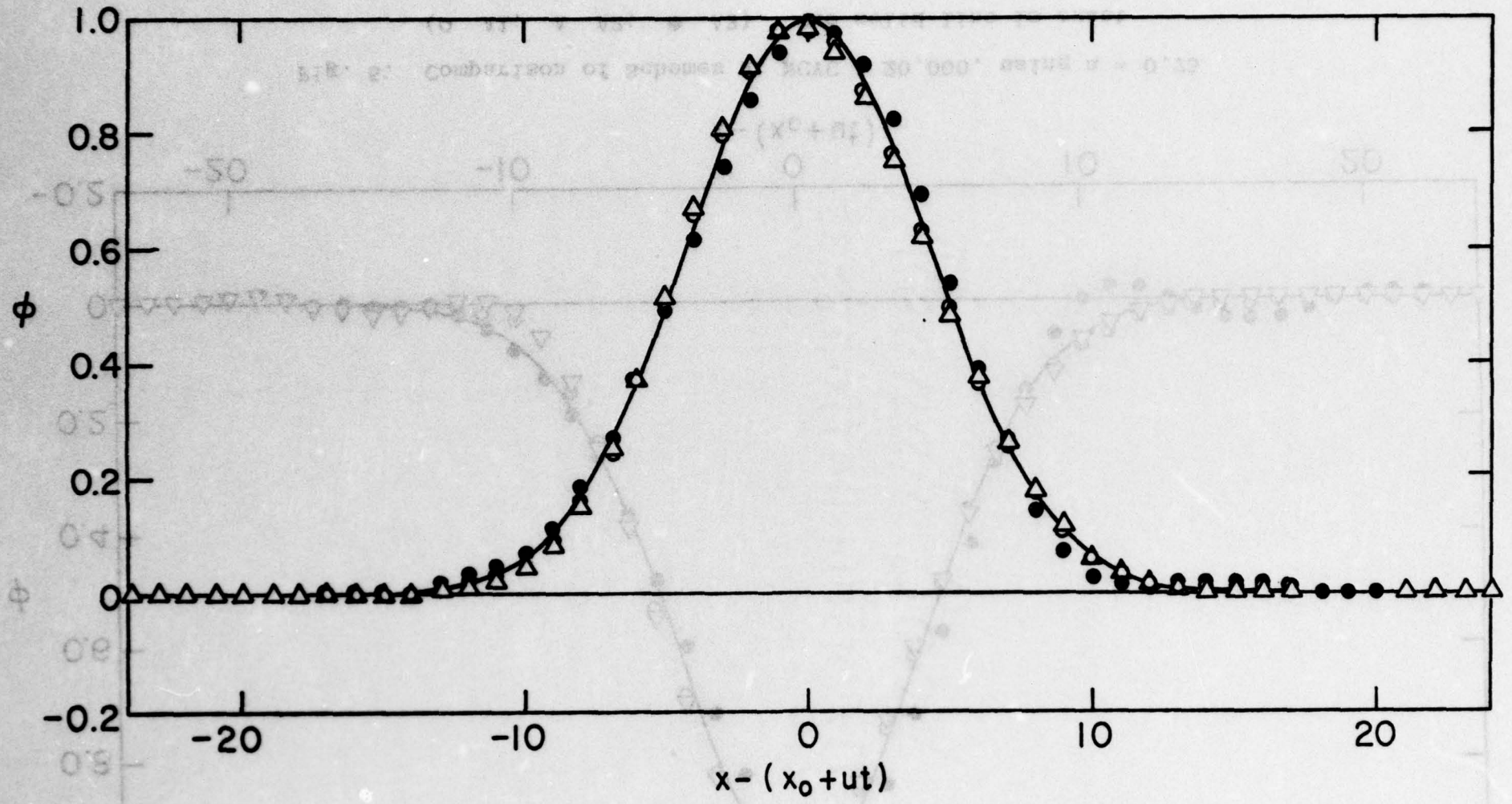

Fig. 4. Comparison of Schemes at NCYC = 10,000, using $\alpha = 0.75$ (O A1; Δ A2; ● A3). The solid line is exact solution.

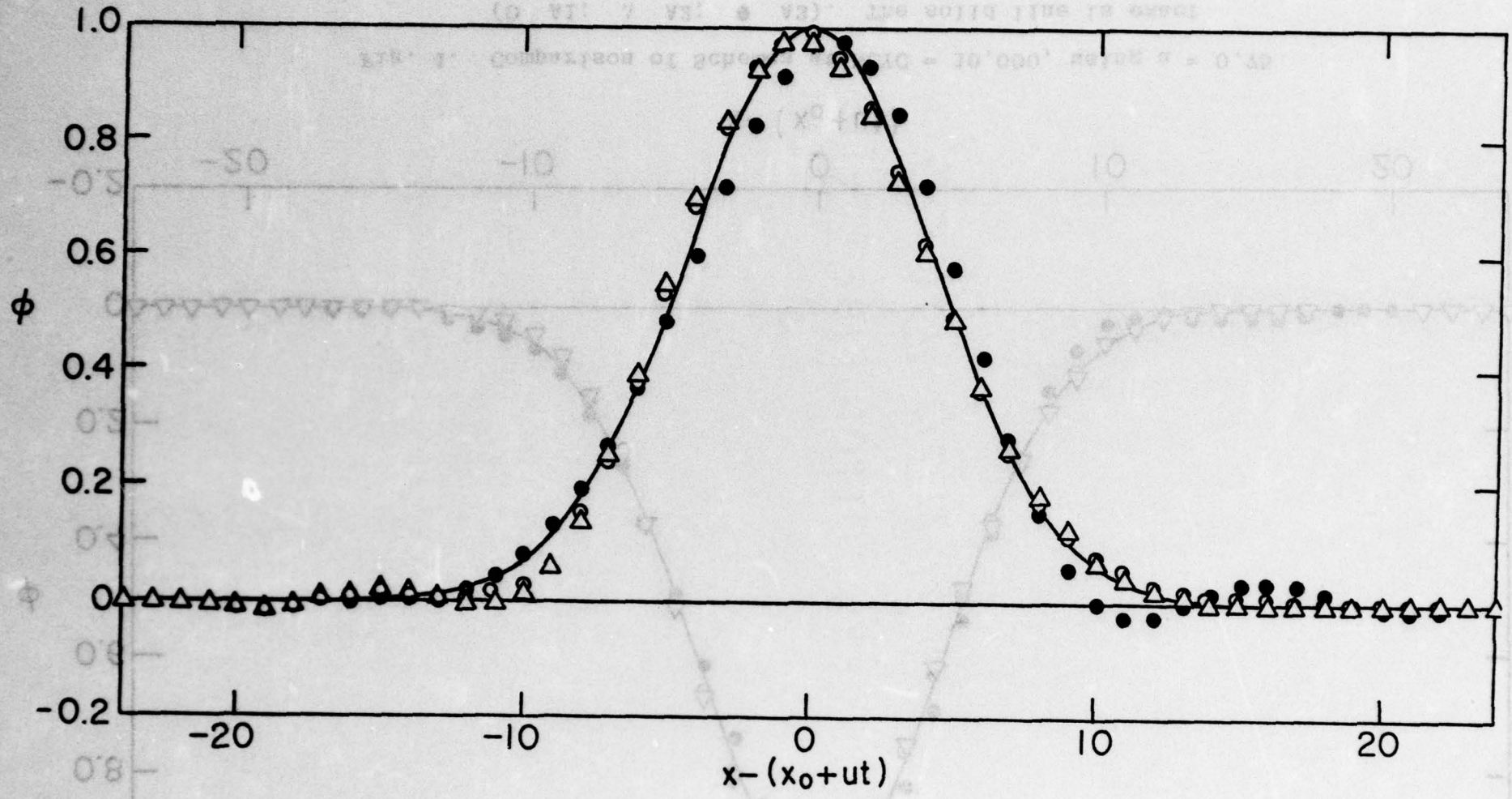

Fig. 5. Comparison of Schemes at NCYC = 20,000, using $\alpha = 0.75$ (O A1; Δ A2; ● A3). The solid line is exact solution.

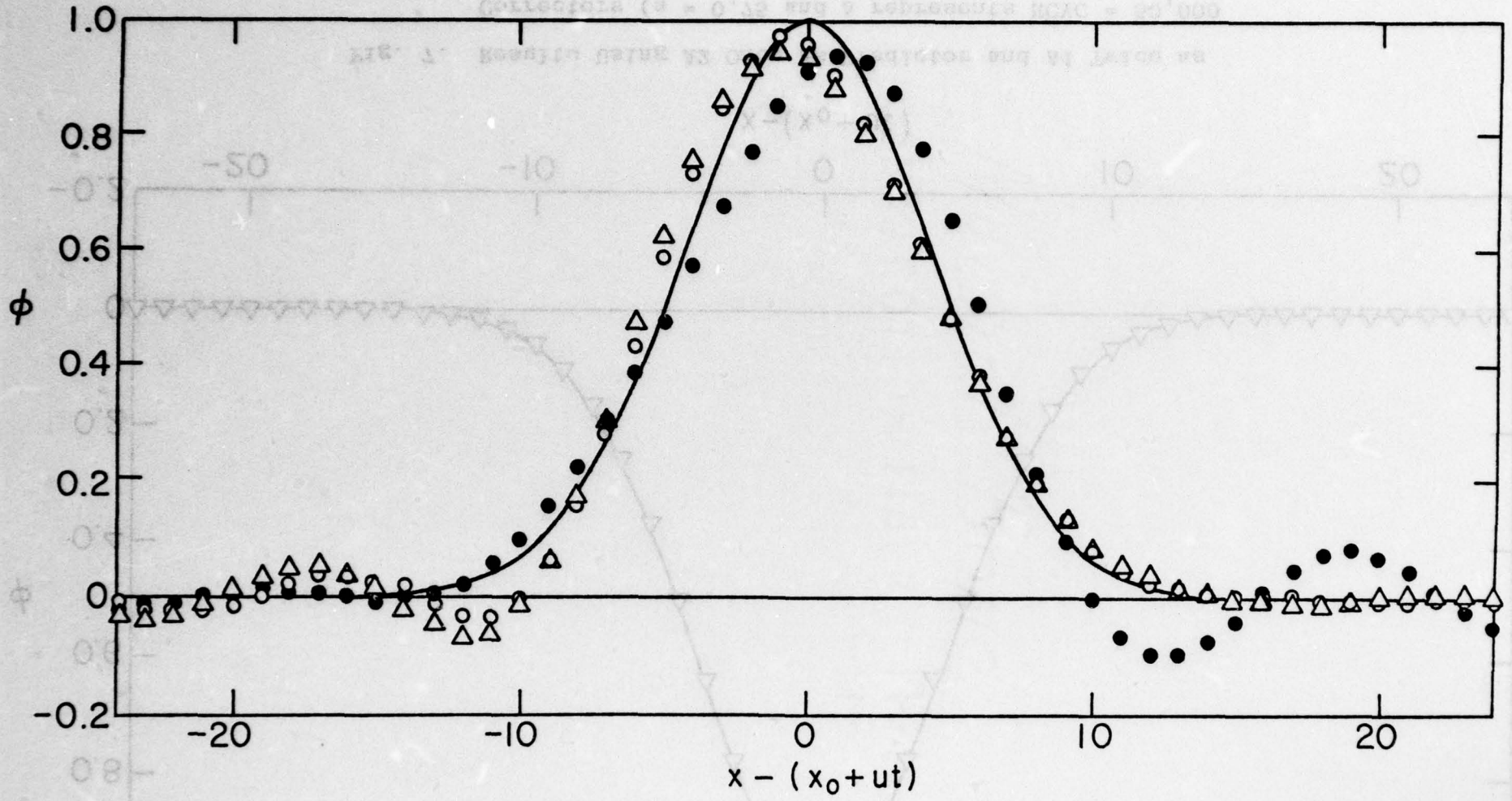

Fig. 6. Comparison of Schemes at NCYC = 50,000, using $\alpha = 0.75$ (O A1; Δ A2; ● A3). The solid line is exact solution.

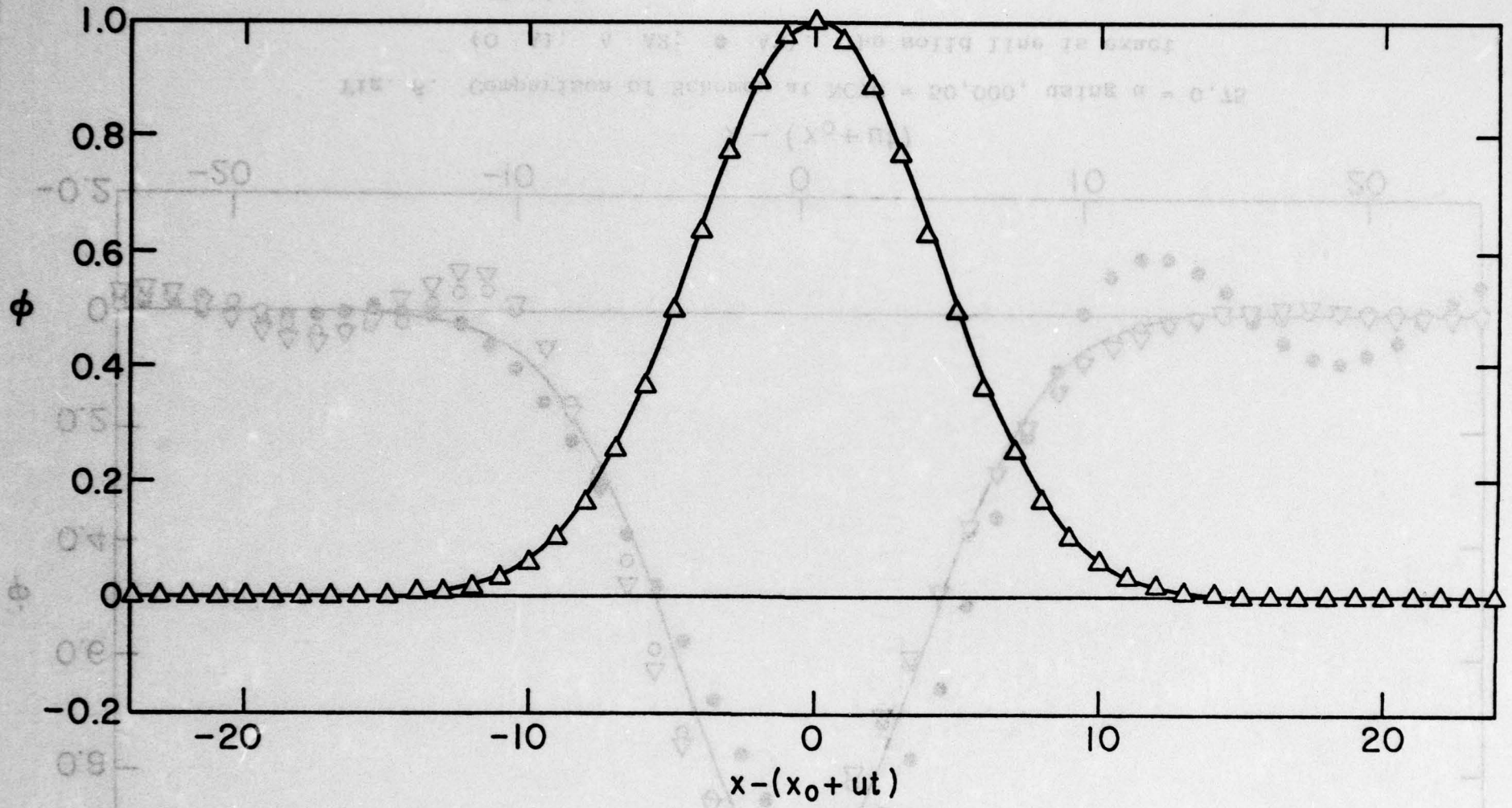

Fig. 7. Results Using A2 Once as Predictor and A4 Twice as Correctors (α = 0.75 and Δ represents NCYC = 50,000 and NCYC = 100,000).

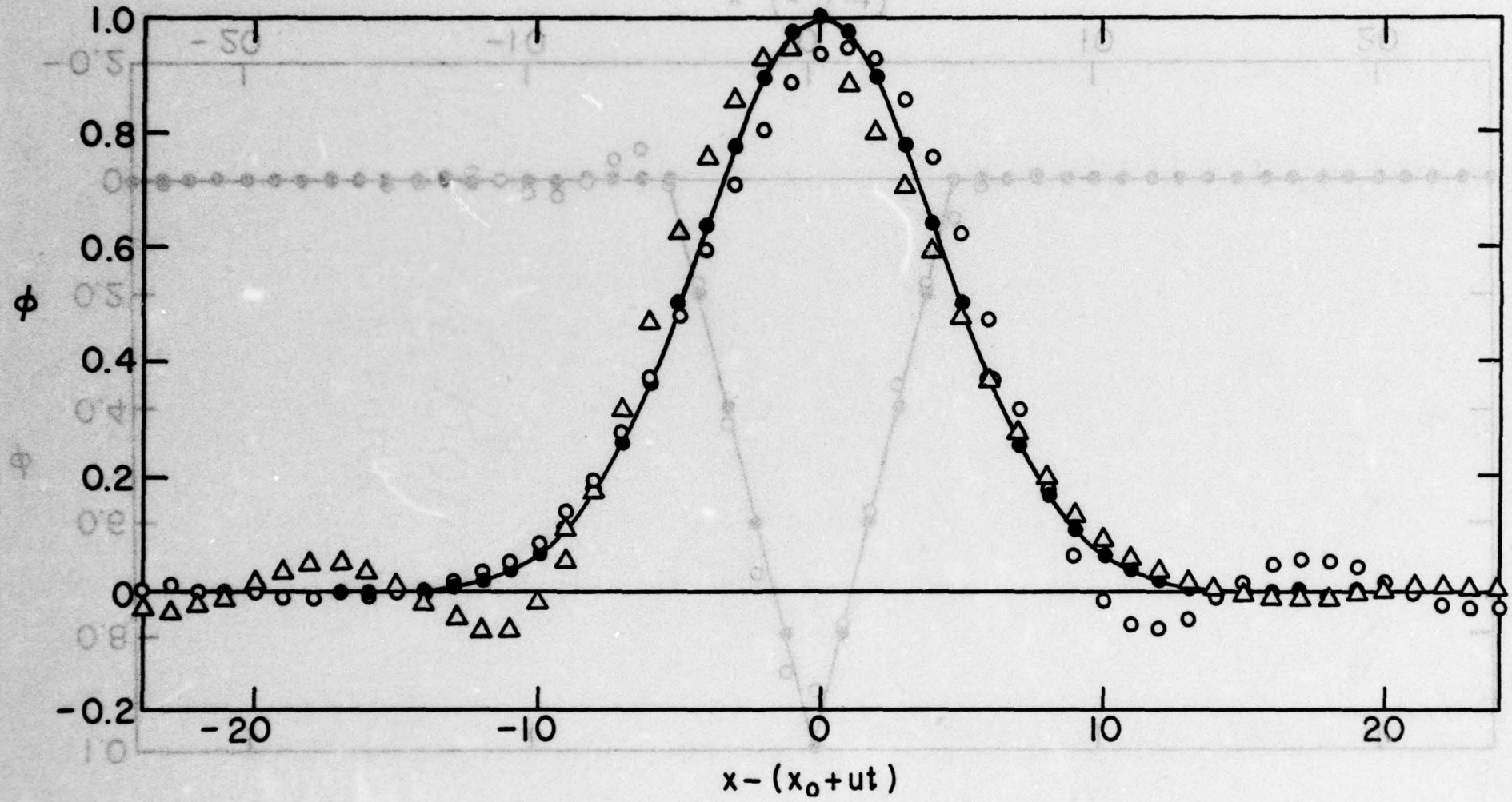

Fig. 8. A2 Results at NCYC = 50,000 (O α = 0.25; ● α = 0.50; Δ α = 0.75).

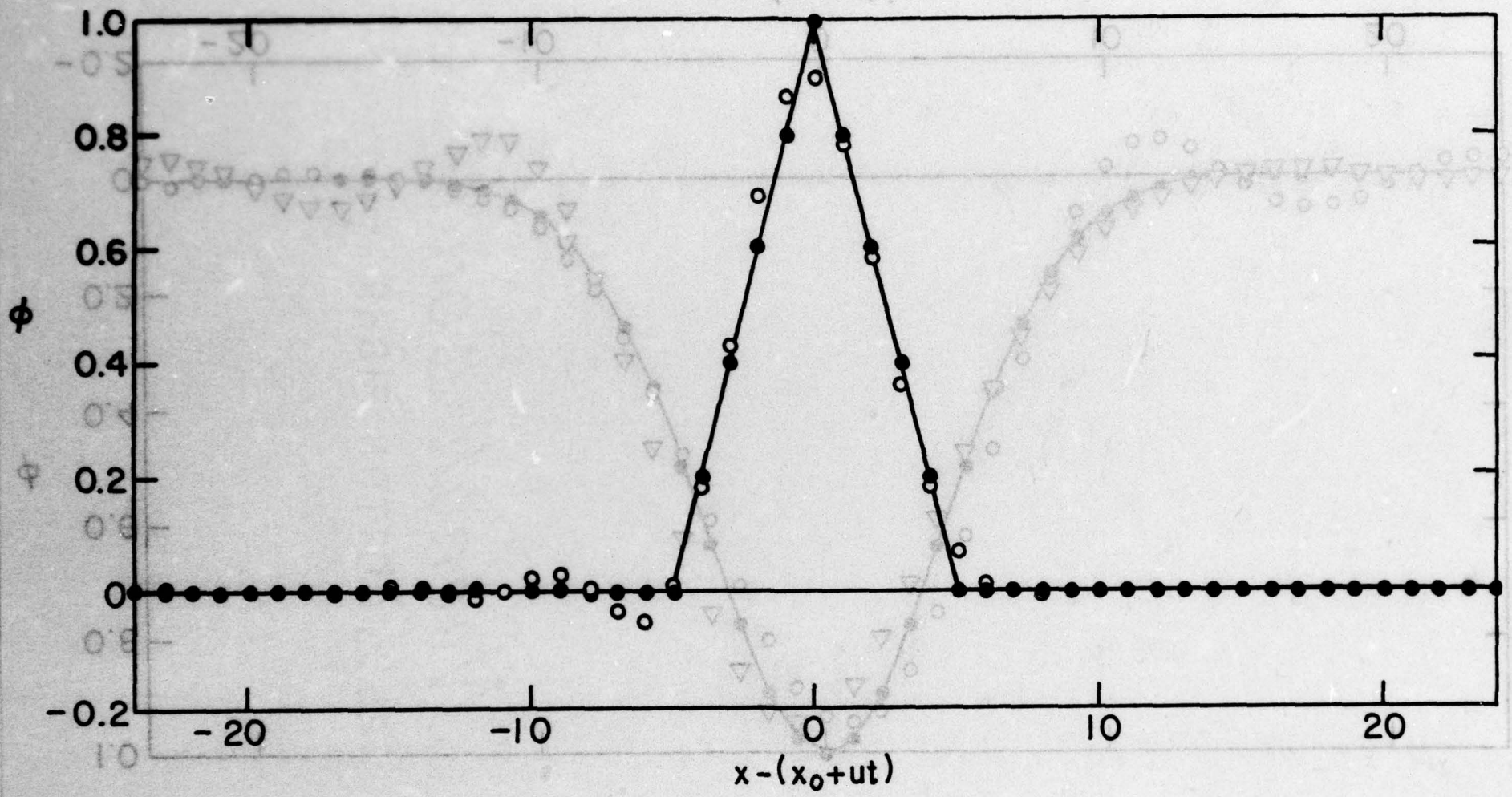

Fig. 9. A2 Results for Triangular Wave at NCYC = 1400

(● α = 0.50; O α = 0.75).

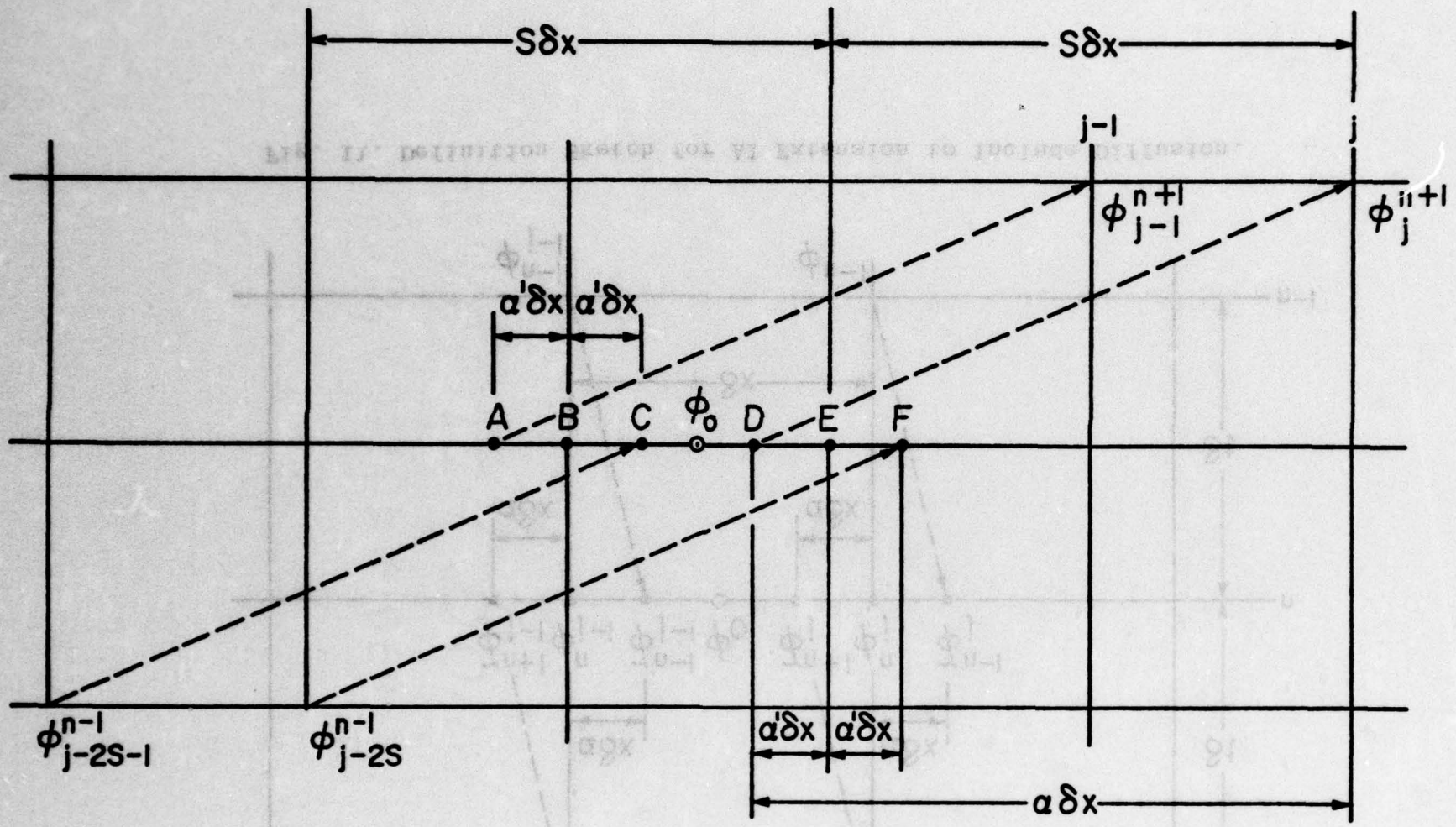

Fig. 10. Definition Sketch for A1 Extension to Arbitrary Courant Number ($\phi_A = \phi^{n+1}_{j-1}$, $\phi_B = \phi^{n}_{j-s-1}$, $\phi_C = \phi^{n-1}_{j-2s-1}$, $\phi_D = \phi^{n+1}_{j}$, $\phi_E = \phi^{n}_{j-s}$, $\phi_F = \phi^{n-1}_{j-2s}$)

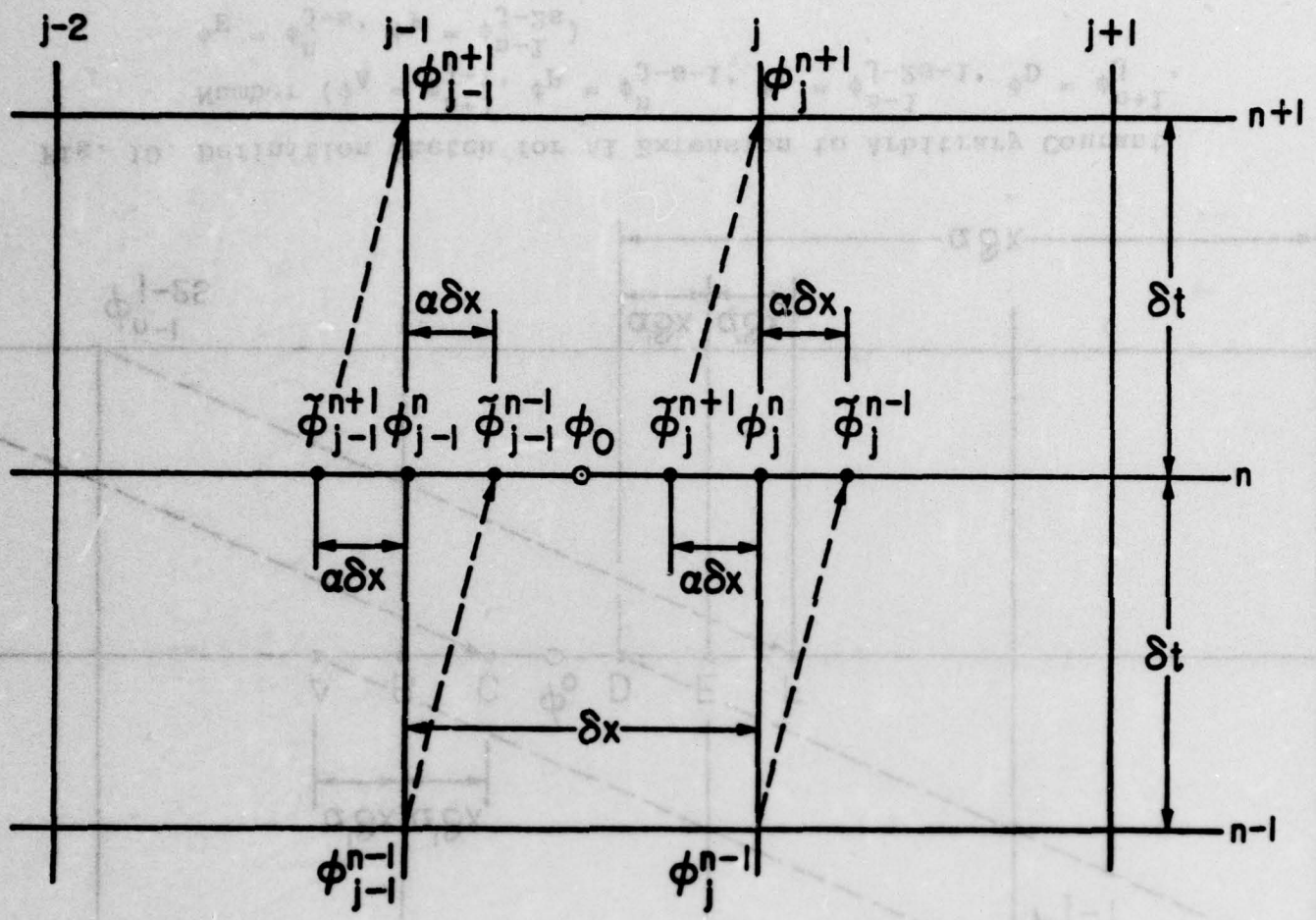

Fig. 11. Definition Sketch for A1 Extension to Include Diffusion.

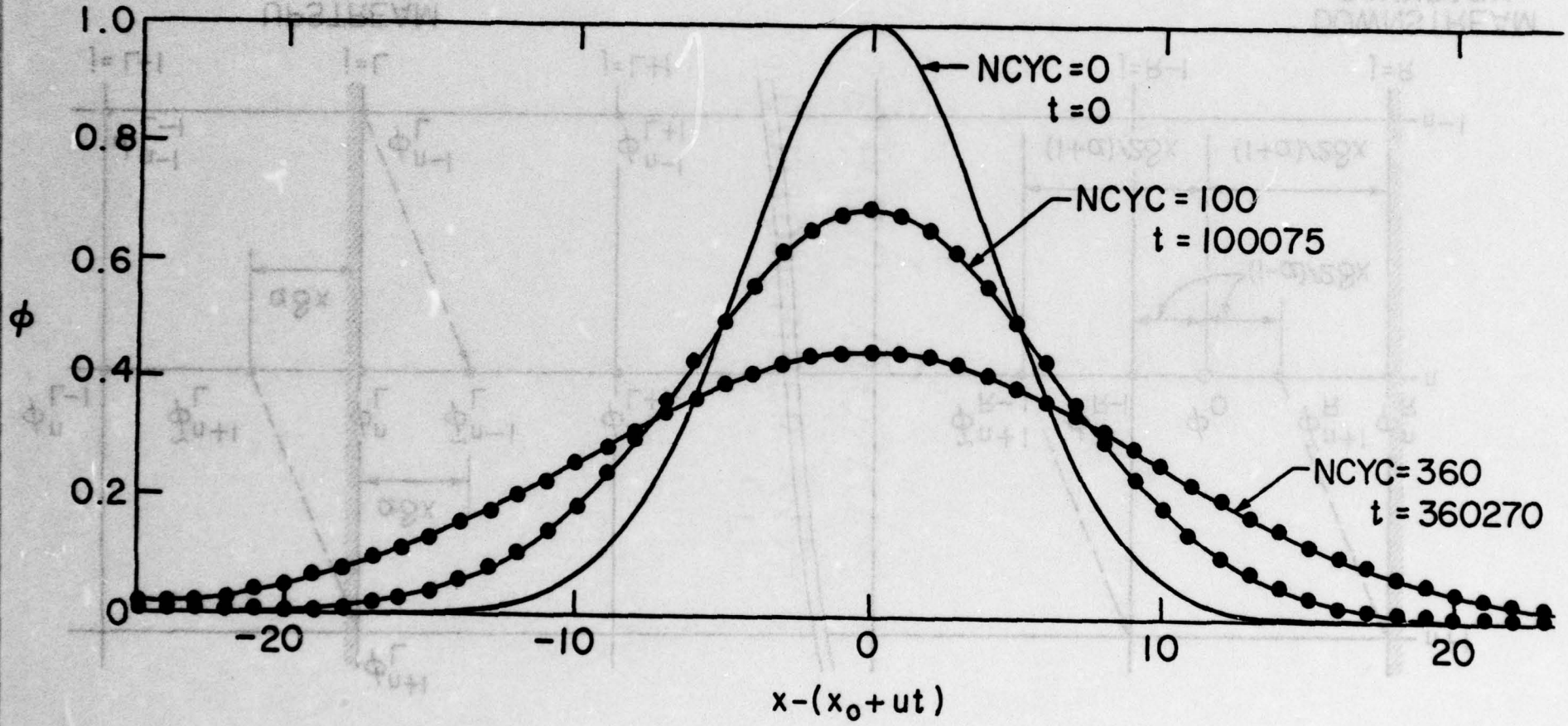

Fig. 12. Comparison of AD1 Results (dots) with Exact Solution (solid lines).

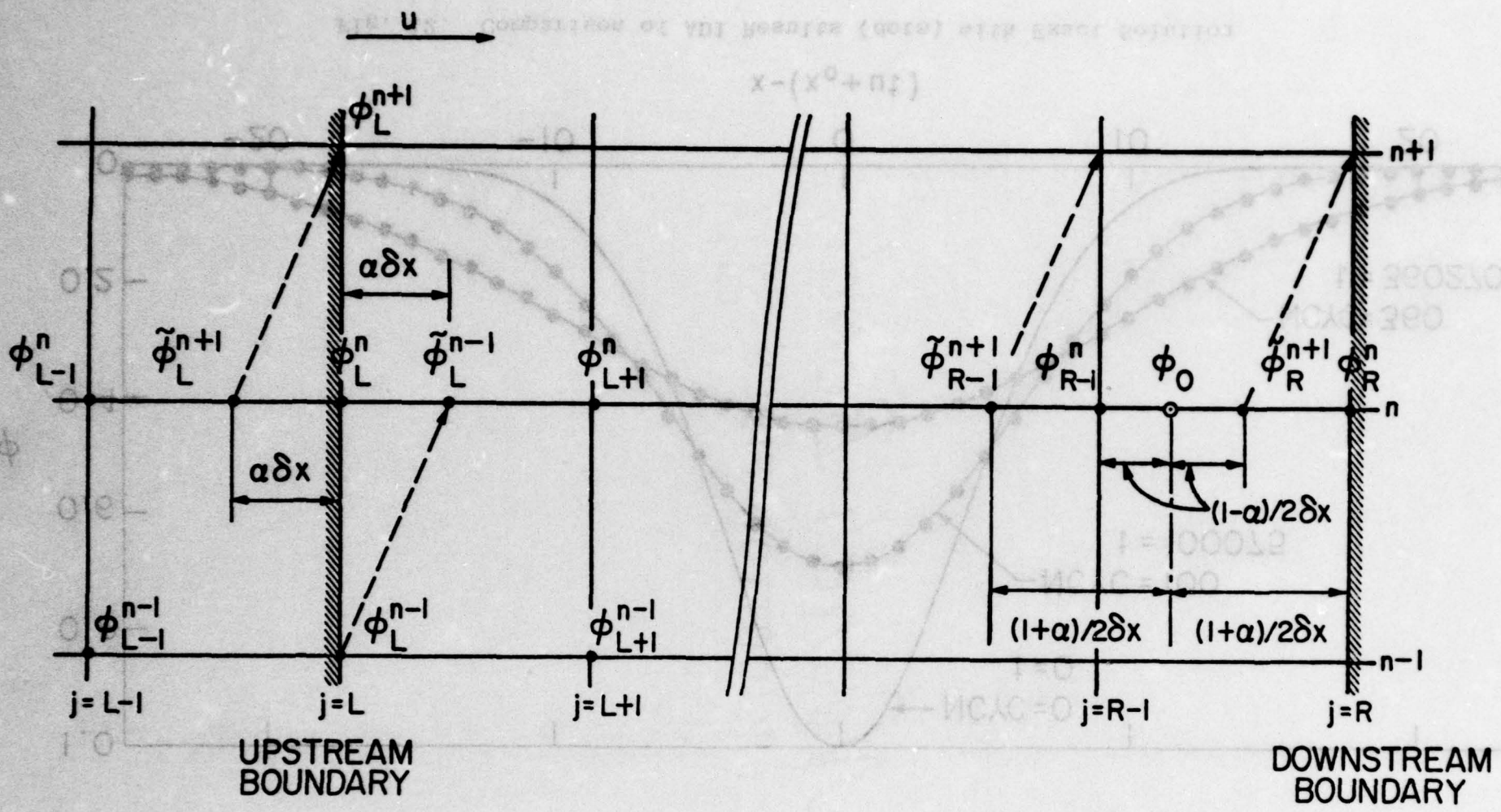

Fig. 13. Definition Sketch for Boundary Conditions.

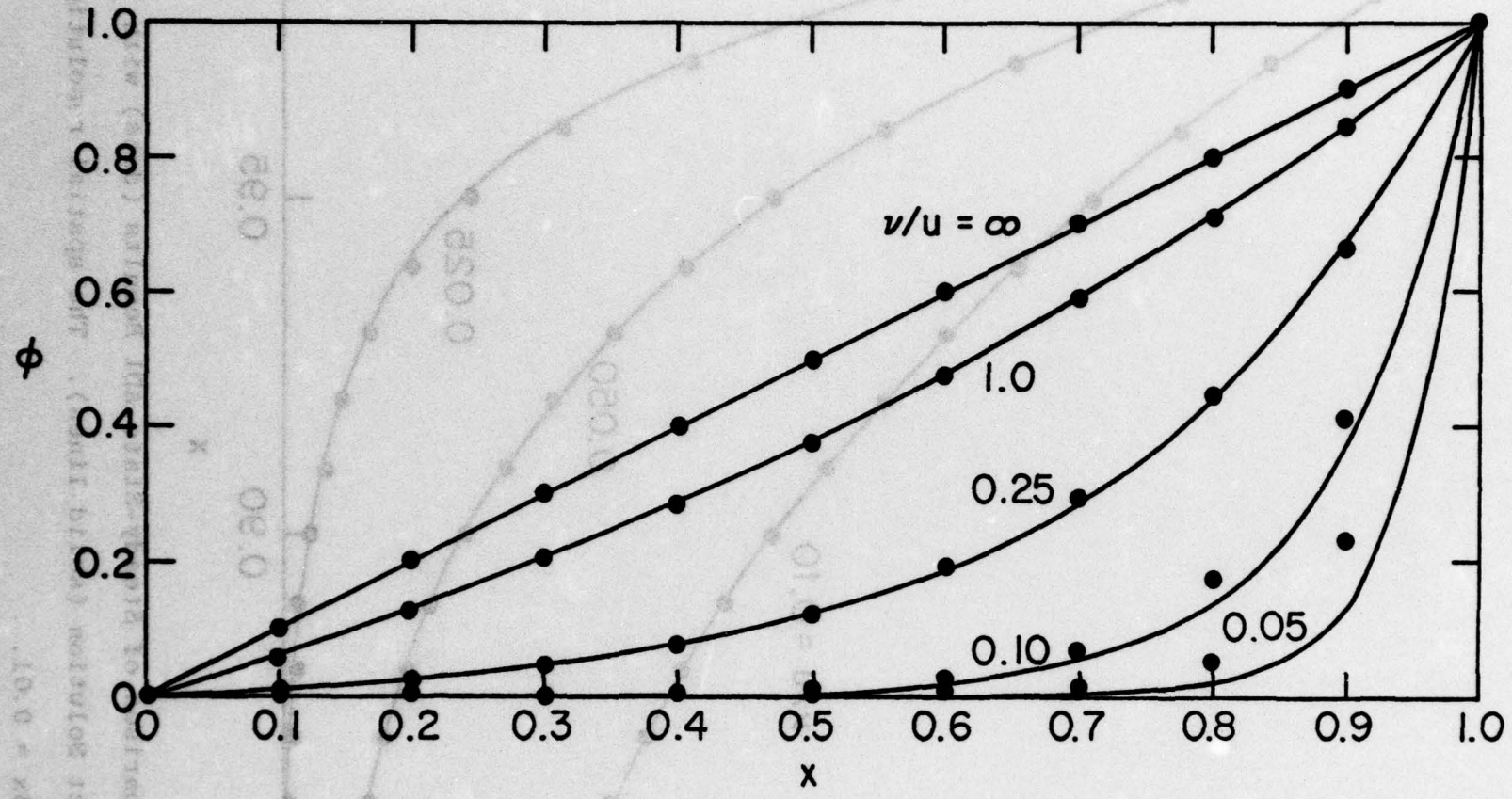

Fig. 14. Comparison of Steady-State AD1 Results (dots) with Exact Solution (solid lines). The spatial resolution is $\delta x = 0.1$.

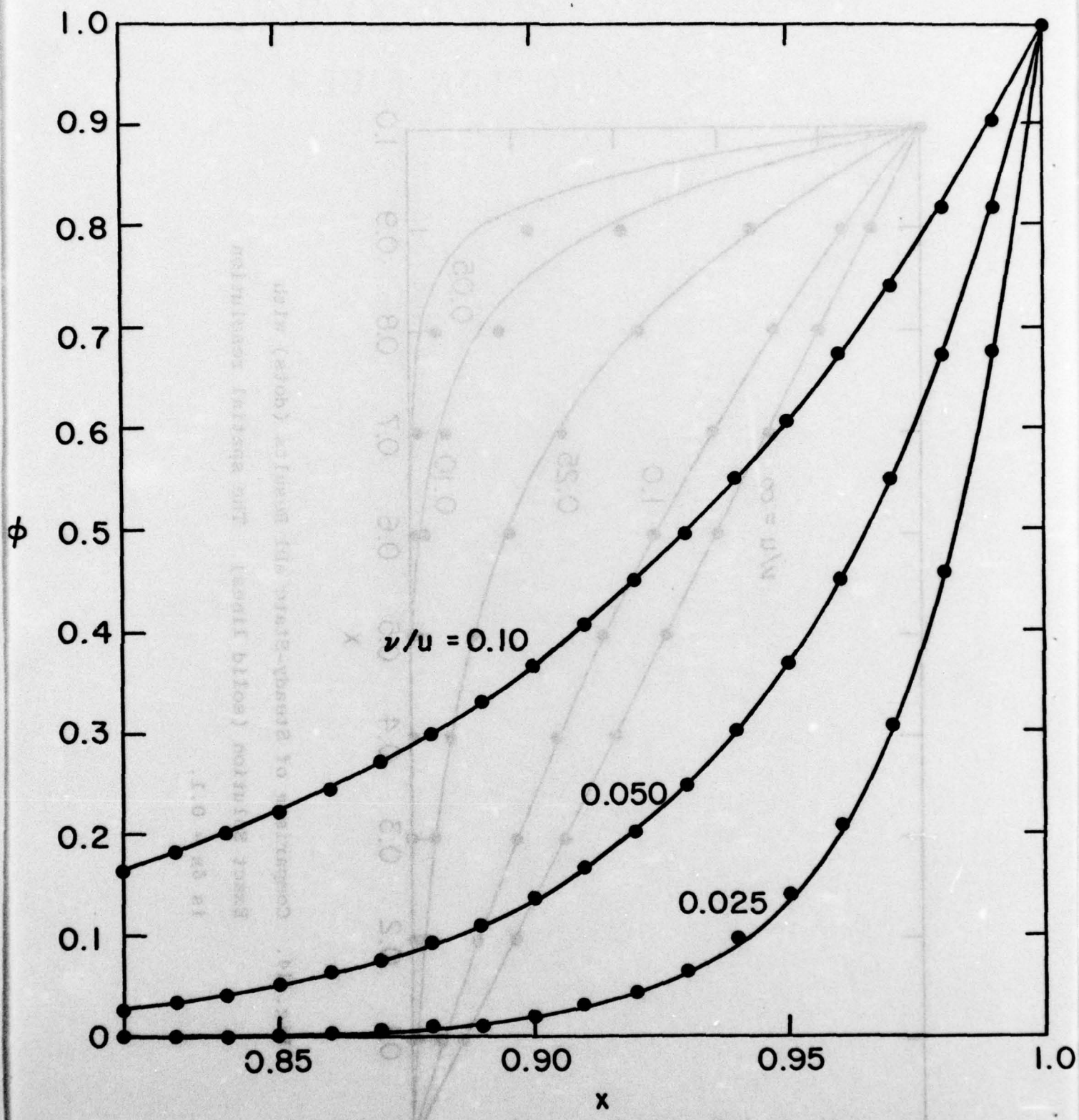

Fig. 15. Comparison of Steady-State AD1 Results (dots) with Exact Solution (solid lines). The spatial resolution is $\delta x = 0.01$.

Unclassified

SECURITY CLASSIFICATION OF THIS PAGE (When Data Entered)

REPORT DOCUMENTATION PAGE

READ INSTRUCTIONS BEFORE COMPLETING FORM

1. REPORT NUMBER

2. GOVT ACCESSION NO.

3. RECIPIENT'S CATALOG NUMBER

4. TITLE (and Subtitle)

A BALANCED EXPANSION TECHNIQUE FOR CONSTRUCTING ACCURATE FINITE DIFFERENCE ADVECTION SCHEMES.

5. TYPE OF REPORT & PERIOD COVERED

Topical rept.,

6. PERFORMING ORG. REPORT NUMBER

J77-7500-TR1

7. AUTHOR(s)

Robert K.-C. Chan

8. CONTRACT OR GRANT NUMBER(s)

N0014-76-C-0455

9. PERFORMING ORGANIZATION NAME AND ADDRESS

JAYCOR
1401 Camino Del Mar
Del Mar, California 92014

10. PROGRAM ELEMENT, PROJECT, TASK AREA & WORK UNIT NUMBERS

NR 062-533

11. CONTROLLING OFFICE NAME AND ADDRESS

Office of Naval Research, Fluid Dynamics Branch
Dept. of the Navy; Arlington, VA 22217

12. REPORT DATE

February 1977

13. NUMBER OF PAGES

49

14. MONITORING AGENCY NAME & ADDRESS (if different from Controlling Office)

50p.

15. SECURITY CLASS. (of this report)

Unclassified

15a. DECLASSIFICATION/DOWNGRADING SCHEDULE

16. DISTRIBUTION STATEMENT (of this Report)

Approved for Public Release; Distribution Unlimited

17. DISTRIBUTION STATEMENT (of the abstract entered in Block 20, if different from Report)

18. SUPPLEMENTARY NOTES

Submitted to *Journal of Computational Physics* for publication.

19. KEY WORDS (Continue on reverse side if necessary and identify by block number)

Advection Schemes
Finite Difference
Computational Fluid Dynamics

20. ABSTRACT (Continue on reverse side if necessary and identify by block number)

A new procedure, called the Balanced Expansion Technique (BET), is employed to construct accurate finite difference advection schemes that, for the model equation considered, are neutrally stable. By applying BET systematically, the phase error can be made as small as one wishes. Test calculations with one-dimensional problems have confirmed the expected accuracy of these methods.

DD FORM 1 JAN 73 1473 EDITION OF 1 NOV 65 IS OBSOLETE

Unclassified

SECURITY CLASSIFICATION OF THIS PAGE (When Data Entered)

392220 SB